Icelandic analogs to Martian flood lavas

Citation for published version:
Keszthelyi, L, Thordarson, T, McEwen, A, Haack, H, Guilbaud, MN, Self, S & Rossi, MJ 2004, 'Icelandic analogs to Martian flood lavas', *Geochemistry, Geophysics, Geosystems*, vol. 5, no. 11, Q11014, pp. 1-32. https://doi.org/10.1029/2004GC000758

Digital Object Identifier (DOI):
10.1029/2004GC000758

Link:
Link to publication record in Edinburgh Research Explorer

Document Version:
Publisher's PDF, also known as Version of record

Published In:
Geochemistry, Geophysics, Geosystems

Icelandic analogs to Martian flood lavas

Laszlo Keszthelyi
Astrogeology Team, U.S. Geological Survey, 2255 North Gemini Drive, Flagstaff, Arizona 86001, USA (laz@usgs.gov)

Thorvaldur Thordarson
Department of Geology and Geophysics, University of Hawaii at Manoa, 2525 Correa Road, Honolulu, Hawaii 96822, USA

Alfred McEwen
Lunar and Planetary Laboratory, University of Arizona, 1629 East University Boulevard, Tucson, Arizona 85721, USA

Henning Haack
Geological Museum, University of Copenhagen, Oster Voldgade 5–7, DK–1350, Copenhagen, Denmark

Marie-Noelle Guilbaud and Stephen Self
Volcano Dynamic Group, Open University, Milton Keynes MK7 6AA, United Kingdom

Matti J. Rossi
Printel OY, Vaino Tannerin tie 3, FIN–01510, Vantaa, Finland

[1] We report on new field observations from Icelandic lava flows that have the same surface morphology as many Martian flood lava flows. The Martian flood lavas are characterized by a platy-ridged surface morphology whose formation is not well understood. The examples on Mars include some of the most pristine lava on the planet and flows >1500 km long. The surfaces of the flows are characterized by (1) ridges tens of meters tall and wide and hundreds of meters long, (2) plates hundreds of meters to kilometers across that are bounded by ridges, (3) smooth surfaces broken into polygons several meters across and bowed up slightly in the center, (4) parallel grooves 1–10 km long cut into the flow surface by flow past obstacles, and (5) inflated pahoehoe margins. The Icelandic examples we examined (the 1783–1784 Laki Flow Field, the Búrfells Lava Flow Field by Lake Myvatn, and a lava flow from Krafla Volcano) have all these surface characteristics. When examined in detail, we find that the surfaces of the Icelandic examples are composed primarily of disrupted pahoehoe. In some cases the breccia consists of simple slabs of pahoehoe lava; in other cases it is a thick layer dominated by contorted fragments of pahoehoe lobes. Our field observations lead us to conclude that these breccias are formed by the disruption of an initial pahoehoe surface by a large flux of liquid lava within the flow. In the case of Laki, the lava flux was provided by surges in the erupted effusion rate. At Búrfells it appears that the rapid flow came from the sudden breaching of the margins of a large ponded lava flow. Using the observations from Iceland, we have improved our earlier thermal modeling of the Martian flood lavas. We now conclude that these platy-ridged lava flows may have been quite thermally efficient, allowing the flow to extend for >100 km under a disrupted crust that was carried on top of the flow.

1. Introduction

[2] The recent discovery that flood lavas on Mars have a surface morphology dissimilar from any well-described terrestrial lava flows has led to a search for suitable terrestrial analogs and a new lava emplacement model [*Keszthelyi et al.*, 2000]. The primary objective of this paper is to report on fieldwork on the best analog we have found: the 1783–1784 Laki flow field in Iceland. We also examined other Icelandic lava flows with similar morphologies. We use these field observations to improve the initial emplacement model we proposed. However, before we describe the terrestrial lavas, we provide a brief discussion of the Martian lavas that provoked this study.

[3] It must also be noted that not all workers agree that these features are lava flows. Mudflows and icebergs are also called upon to form the surfaces of the young plains and channel floors. Specifically, *Rice et al.* [2002, 2003] and *Williams and Malin* [2004] both argue that "lava" features seen on the floors of some Martian flood channels are more likely to have formed as a combination of mud and ice flowed over the surface. *Woodworth-Lynas and Guigné* [2003] argue that many of the features that *Keszthelyi et al.* [2000] interpret to be lava features could have formed when icebergs rested on the plains of Mars. These workers make interesting arguments that we do not try to refute here. Instead, our goal is to present a compelling case that the Martian features could indeed be lava flows. Only continued exploration of Mars will decide this question.

2. Mars

2.1. Overview of Martian Geologic History and the Role of Flood Lavas

[4] At its most basic, the geology of Mars is defined by a dichotomy between the heavily cratered southern highlands and the smooth northern plains (Figure 1). This dichotomy may have been formed by a giant impact late in the accretion of Mars (~4.5 Ga), a cluster of impact basins, or endogenic processes [e.g., *Frey and Schultz*, 1988;

McGill and Dimitriou, 1990; *Lenardic et al.*, 2004]. Soon afterward (presumably ~4–3.8 Ga, by analogy to the Moon), heavy meteorite bombardment produced large impact basins across both hemispheres of Mars [e.g., *Frey et al.*, 2002]. Later processes have filled the northern plains with a few kilometers of deposits, producing the relatively smooth surface we see today [*Scott and Tanaka*, 1986; *Tanaka and Scott*, 1987; *Greeley and Guest*, 1987; *Head et al.*, 2002; *Tanaka et al.*, 2003].

[5] The other global-scale geologic feature on Mars is the Tharsis bulge (Figure 1). This is a region that has had sustained volcanism for much of Mars' geologic history, building a plateau standing ~4 km above its surroundings. On this plateau stand five massive shield volcanoes, including the largest volcano in the Solar System, Olympus Mons. The weight of the Tharsis bulge has affected the lithospheric stress pattern across much of Mars [e.g., *Arkani-Hamed and Riendler*, 2002]. A smaller group of shield volcanoes is centered around Elysium Mons (Figure 1).

[6] Flood volcanism seems to have played an important role throughout Mars' geologic history. The heavily cratered southern highlands of the oldest period on Mars, the Noachian Period, are generally assumed to have originally been volcanic plains, but the impacts have obliterated most of the diagnostic lava features [e.g., *Scott and Tanaka*, 1986; *Greeley and Guest*, 1987]. Supporting evidence comes from the fact that the southern highlands have infrared spectra consistent with relatively unaltered basalt [e.g., *Christensen et al.*, 2000, 2003]. The nature of the ancient surface of Mars can be seen in the 4–10 km cross-sections of the crust seen in the giant Valles Marineris canyon system. The layering in the walls of these canyons is often morphologically similar to the step-like layers seen in eroding terrestrial flood basalt provinces [*McEwen et al.*, 1999]. However, there are also many layers with morphologies suggestive of pyroclastic deposits and/or thin lava flows [*Beyer*, 2004]. During the middle period of Mars' geologic history, the Hesperian Period, flood lavas appear to have helped cover the northern plains, burying the ancient impact basins [*Head et al.*, 2002]. There are also extensive areas mapped
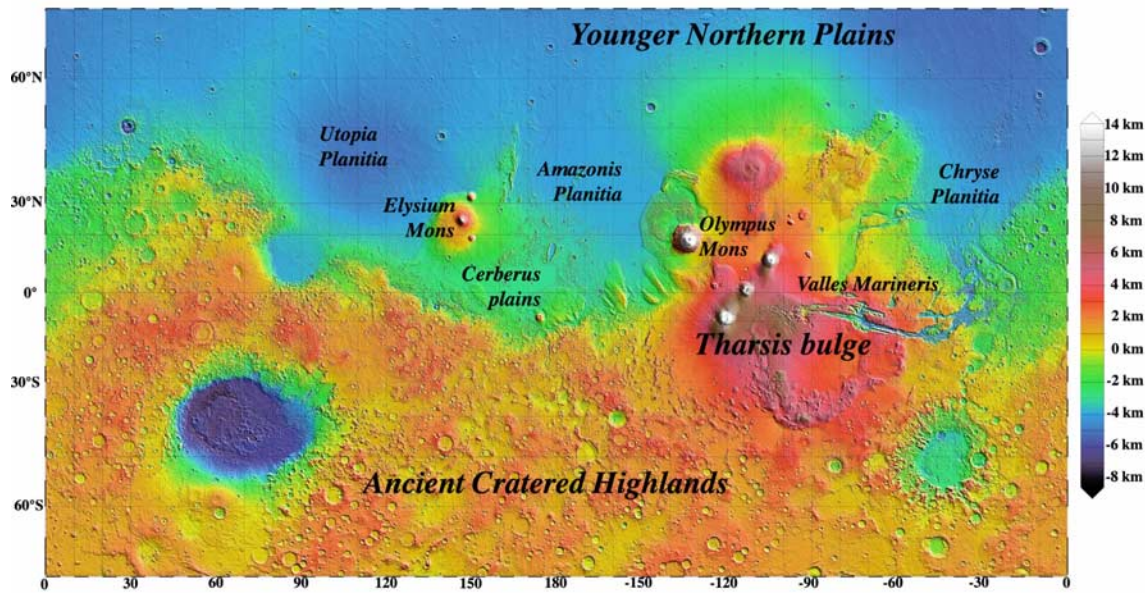
Figure 1. Mars Orbiter Laser Altimeter (MOLA) map of Mars with major physiographic features labeled. Recent flood lavas are seen in the Cerberus plains and Amazonis Planitia, as well as on the Tharsis Bulge. Flood lavas also appear to outcrop in the walls of Valles Marineris. While obscured by secondary processes (especially eolian cover and impacts), it is plausible that much of the northern plains are underlain by flood lavas, and it is possible that much of the original surface of the ancient southern highlands was produced by flood volcanism. Thus it appears that flood volcanism is a far more widespread process on Mars than the shield volcanism that has produced edifices such as Olympus Mons and Elysium Mons.

as Hesperian ridged plains, which most workers think are flood lavas [e.g., *Tanaka*, 1986]. During the most recent period, the Amazonian Period, flood lavas covered large areas of the Tharsis and Elysium regions. Flood lavas in the Upper Amazonian have been documented in Amazonis Planitia [e.g., *Keszthelyi et al.*, 2000; *Fuller and Head*, 2002; *Tanaka et al.*, 2003; *Lanagan and McEwen*, 2004] and following some of the channels extending northeast from Tharsis toward Chryse Planitia (Figure 1). Furthermore, many of the youngest lava flows on Olympus Mons are covered by flood lavas at the base of the shield volcano. There is also compelling evidence that flood volcanism has continued into very recent times (<200 Ma) in the Cerberus plains (Figure 1).

[7] Dating the most recent flood lavas [e.g., *Hartmann and Berman*, 2000; *Burr et al.*, 2002] has been controversial because the origin, rate of production, and degradation of small craters are poorly understood. The dearth of craters on many recent lava surfaces indicates a surface exposure age of <10 Ma according to the production function of *Hartmann and Neukum* [2001]. However, A. S. McEwen et al. (The

rayed crater Zunil and interpretations of small impact craters on Mars, submitted to *Icarus*, 2004) (hereinafter referred to as McEwen et al., submitted manuscript, 2004) argue that this production function is incorrect and that the majority of small craters (<500 m diameter) on Mars are secondary craters. More conservative approaches, using larger craters, indicate that there is a package of lava flows in the Cerberus plains that is ~100 ± 50 Ma in age [*Plescia*, 1990, 2003; *Lanagan and McEwen*, 2004]. This is the youngest large-scale bedrock currently known on Mars. Thus, while it is difficult to place absolute ages on these young lavas, there is evidence of widespread flood volcanism in the northern hemisphere of Mars continuing through the most recent geologic period of Mars.

[8] It is interesting to note that the ~100 Ma age for the Cerberus plains is consistent with the radiometric ages of the youngest meteorites [*Nyquist et al.*, 2001]. In fact, McEwen et al. (submitted manuscript, 2004) suggest that some of the basaltic shergottite meteorites originated from the Zunil impact in the Cerberus plains. If this suggestion is correct, we have a sample of these Martian flood lavas. The average bulk

Table 1. Average Bulk Composition of Four Shergottite Meteorites[a]

Meteorite	EET 79001	Shergotty	QUE 94201	Zagami
SiO_2	49.65	51.30	47.90	50.50
TiO_2	0.94	0.82	1.84	0.79
Al_2O_3	8.56	6.88	11.00	6.05
FeO	17.90	19.40	18.50	18.10
MnO	0.48	0.52	0.50	0.49
MgO	11.34	9.30	6.25	11.30
CaO	9.03	9.60	11.40	10.50
Na_2O	1.30	1.39	1.58	1.23
K_2O	0.06	0.17	0.04	0.14
P_2O_5	0.94	0.67	–	0.19

[a] Data from *Lodders* [1998]. The two EET 79001 meteorites were averaged. The meteorites have variable petrology and alteration. However, comparison to the Laki lava flow (Table 2) shows that these Martian basalts are not extremely dissimilar from typical terrestrial basalts.

composition of four basaltic shergottite meteorites is shown in Table 1. These lavas are somewhat iron rich, but are otherwise broadly similar to terrestrial basalts. There is no reason to suspect that Martian basalts would have behaved very different from terrestrial ones.

2.2. Lava Morphology

[9] Details of the lava morphology can be best seen where the lavas are best preserved. This is in the Cerberus plains. The young lavas in Cerberus are interleaved in a complex manner with aqueous floods, tectonics, and mantling deposits (Figure 2). Recently, the young fluvially carved channel systems at Athabasca, Grjotá, Rahway, and Marte Valles have attracted the greatest interest. These
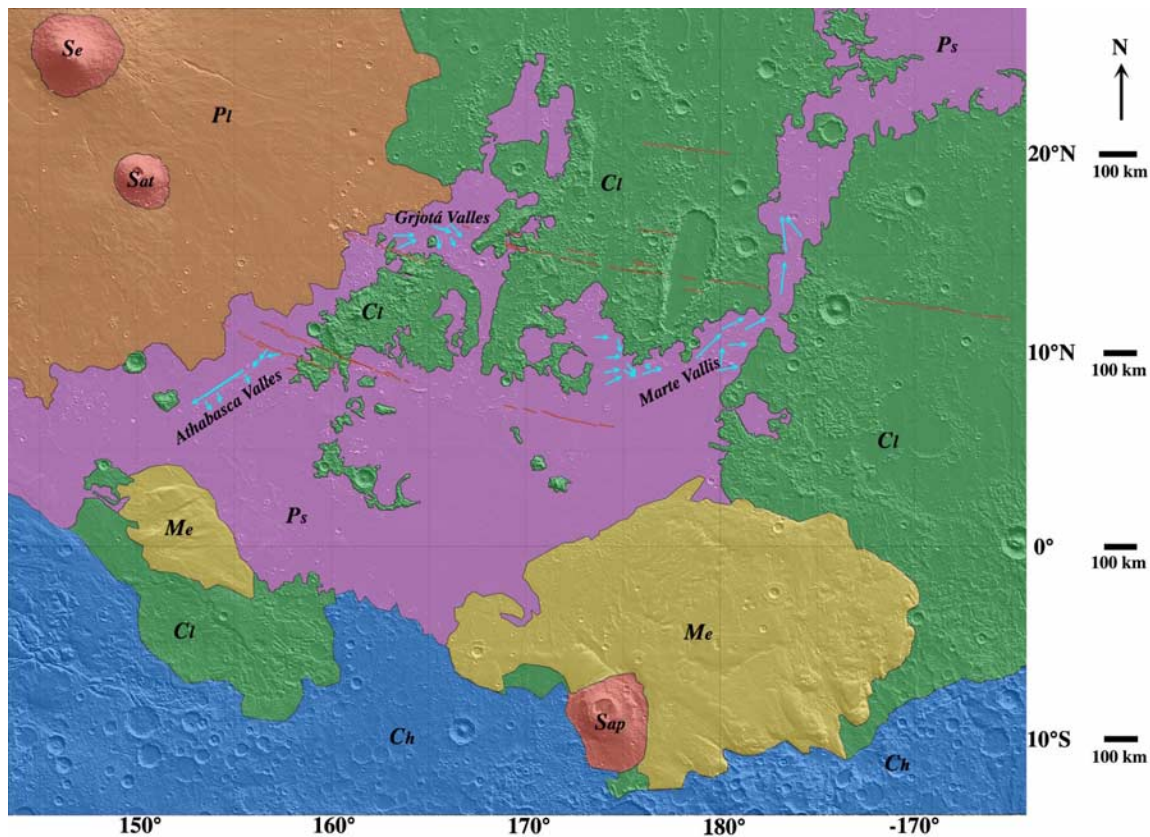

Figure 2. Geomorphologic sketch map of the Cerberus plains region of Mars based on MOLA topography. S denotes shield volcanoes, C cratered terrain, M mantling deposits, and P plains. Se is the Elysium Mons shield volcano, Sat is Albor Tholus, and Sap is Apollinaris Patera. Ch is the cratered highlands, and Cl is cratered lowlands. Me is a mantling deposit that is eroding via eolian processes and generally corresponds to the Medusae Fossae Formation. Pl indicates plains with lobate lava flows, mostly emanating from around Elysium Mons. Ps indicates smooth plains, generally interpreted to be recent flood lava flows. Red lines show the location of major tectonic fissures, collectively referred to as the Cerberus Fossae. Blue arrows show the locations of channels carved by aqueous floods. These are concentrated in three areas: Athabasca Valles, Marte Vallis, and Grjotá Valles.
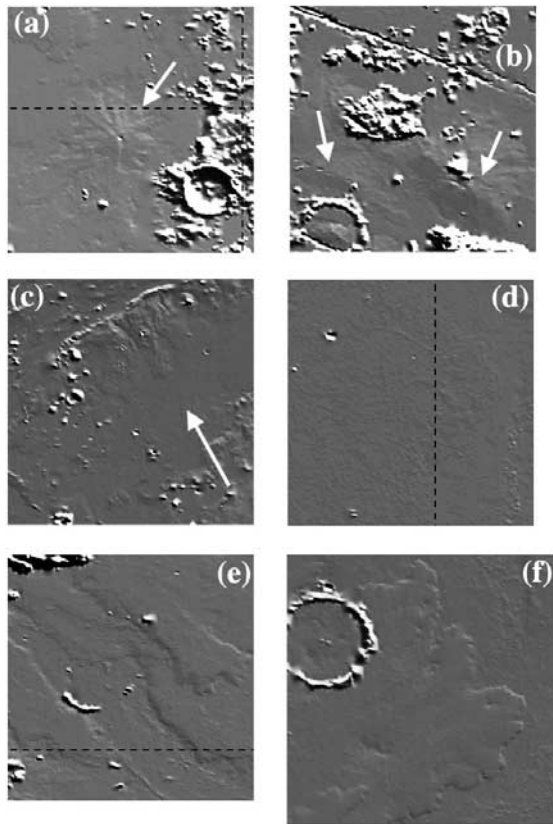
Figure 3. Detailed MOLA topography from different parts of young Martian flood lavas. Each cutout is 150 km on each side; north is to the top in all cases. Shaded relief maps stretched to make topographic features ~10 m tall visible. (a) Very low shield volcano embayed by later flood lavas at approximately 0°N, 160°E. While several low shields are visible in the Cerberus plains, they do not appear to be the source for the flood lavas. (b) Possible source region for some flood lavas along the Cerberus Fossae fracture system at approximately 8°N, 167°E. Arrows show elongated mounds parallel to the tectonic fractures that could be vents that have been buried by the last stages of the eruption. (c) Smooth plains characteristic of the most pristine flood lavas around 7°N, 153°E. (d) Minimal topography that appears to correlate to plates of lava that have been pulled apart around 2°S, 165°E. (e) Lobate margins of relatively short (~400 km long) lava flows in the Cerberus plains near 6°N, 163°E. (f) Lobate margins of >1500 km long lava flows that traversed the length of Marte Vallis and terminate within Amazonis Planitia. Terminus near 27°N, 192°E.

channels contain streamlined landforms and other geomorphologic indicators of the passage of catastrophic aqueous floods [*Burr et al.*, 2002; *Plescia*, 2003]. Superposition and other relations suggest that aqueous floods and lava flows were interleaved in time [*Burr et al.*, 2002; *Plescia*, 2003].

Tectonic features in the area include fissures opened in tension and wrinkle ridges formed in compression. The fissures form a >1500 km long, roughly east-west trending, subparallel set of fractures named the Cerberus Fossae. Wrinkle ridges oriented perpendicular to the Cerberus Fossae are seen across most of Cerberus plains. In some locations, the fissures appear to cut the young lavas and in other areas, the lavas appear to cover sections of the fissure [*Berman and Hartmann*, 2002; *Plescia*, 2003; *Lanagan and McEwen*, 2004], indicating that volcanism and tectonism was interleaved. The orientations of the tectonic features are consistent with control based on lithospheric loading from the Tharsis bulge. Mantling deposits, such as the Medusae Fossae Formation on the southern border of the Cerberus plains (Figure 2), can also be seen to overlie and to be overlain by recent lava flows [*Lanagan and McEwen*, 2004]. We will focus on the lava flows within the Cerberus plains, but the complex geologic history of the region cannot be completely ignored.

[10] In general, it appears that the Cerberus flood lavas (and water floods) were erupted from the Cerberus Fossae fissure system [*Burr et al.*, 2002; *Plescia*, 2003]. Modeling has shown that these fissures could be formed by magmatic dikes that crack the cryosphere and allow floods of both water and lava to erupt from the fissures [*Head et al.*, 2003]. Alternatively, *Burr et al.* [2002] suggest that these fissures are primarily tectonic and that both magma and groundwater have taken advantage of these weaknesses in the lithosphere at different times. The lack of clear evidence for magma-water interaction along the Cerberus Fossae leads us to prefer the *Burr et al.* [2002] model. However, significant additional work is needed to produce a conclusive model for how the fissures, magmas, and waters interact.

[11] There are also very shallow shields and ridges that generally follow the trend of the Cerberus Fossae that were sources of some lava flows (Figures 3a and 3b) [*Plescia*, 2003]. These shields and ridges are mostly a few tens of meters tall and a few tens of kilometers in radius [*Plescia*, 2003]. Thus, slopes on these topographic features are only of the order of 0.1%. It is a true testament to the precision of the Mars Orbital Laser Altimeter (MOLA) that such subtle features can be so clearly seen [e.g., *Kreslavsky and Head*, 2000]. In visible and infrared images, it is extremely difficult to find conclusive morphologic evidence that lava ema-
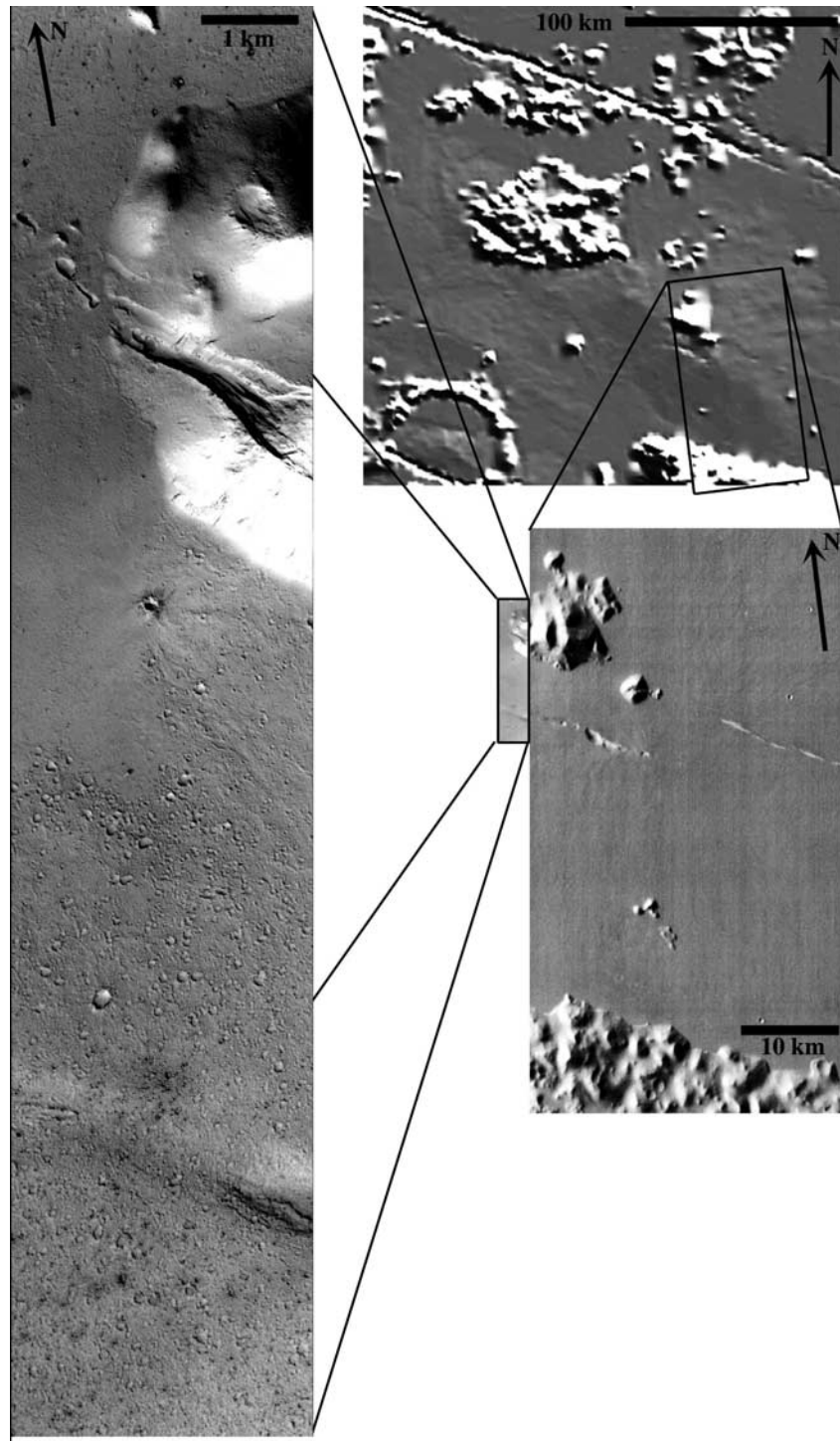
Figure 4. Details from a possible vent region for Cerberus flood lavas. Top right is a 150 × 150 km region of MOLA shaded-relief topography as in Figure 3b. Bottom right is a 100 m/pixel THEMIS daytime thermal infrared view of one of the raised regions along the Cerberus Fossae. This section of the fissure system has been interpreted as a possible source region for flood lavas. The image is contrast enhanced to highlight very subtle temperature variations that are consistent with (but not diagnostic of) radial lava flows covered with a few centimeters of dust. The region adjacent to the THEMIS image is shown to the left in a 5 m/pixel Mars Orbital Camera (MOC) image. No volcanic features are obvious, but the area adjacent to the fissures has had a relatively recent deposit that has covered the older cratered surface. The crenulations and undulations in this more recent deposit are consistent with, but not diagnostic of, lavas covered with a thin deposit of eolian materials. These data show how difficult it is to positively identify the sources of the Martian flood lavas. MOC image number E1104266 and THEMIS IR image I03814010.

nated from these fissures (Figure 4). There are a few cases in which small (kilometer-scale) flows are seen surrounding strands of the Cerberus Fossae [*Plescia*, 2003; *Lanagan and McEwen*, 2004], but these are very rare.

[12] Both the lavas and the water floods traveled down the same topography. In general, this takes fluids south from the Cerberus Fossae and then out to Amazonis Planitia through the northeast trending Marte Vallis (Figure 2). While channels carved by floodwaters can be seen in several parts of the Cerberus plains, the bulk of the plains are covered by essentially unmodified flood lavas and are exceptionally flat (Figures 3c and 3d). In fact, the average slope across the Cerberus plains is only 0.02–0.04% [*Kreslavsky and Head*, 2000; *Plescia*, 2003; *Lanagan and McEwen*, 2004]. The greatest topography related to lava flows is seen at the flow margins. In all cases that they are visible, the flow margins are only a few tens of meters tall and exhibit a lobate trace.

[13] The bulk of the flood lava surfaces are characterized by a combination of plates and ridges (Figures 5–7), leading to the name "platy-ridged lava" being applied to them [*Keszthelyi et al.*, 2000]. The plates are typically about a kilometer in diameter and can have a smooth or a rough surface. In some cases, the plates can be fit together in a "jigsaw puzzle" and can be used to infer flow direction (Figures 5 and 7). Flow is (unsurprisingly) consistently downhill in the cases we have examined. In other locations, the plates are covered with sub-parallel, arcuate, undulating ridges reminiscent of folds seen on the brecciated flow tops of rhyolite flows or basaltic aa flows (Figures 6 and 7). The size of the ridges on these surfaces is quite variable, but in general they are ~10 m tall, on the basis of shadow measurements [*Lanagan and McEwen*, 2004], have a wavelength of several tens of meters and extend for a few hundred meters [*Keszthelyi et al.*, 2000].

[14] The region between the plates can also be smooth or ridged (Figures 5–7). When the plate surface is smooth, it is most common to have narrow ridges bounding the plates (Figures 5 and 6). These ridges are inferred to have formed by compression where plates collided against each other and we refer to them as "pressure ridges." Where the plates appear to have rafted apart, the surface is usually smooth and slightly lower topographically (Figures 5e and 7). These smooth "inter-plate" areas often are marked by 10-m scale polygons (Figure 5f). Using the shading seen on

these polygonal surfaces, *Lanagan and McEwen* [2004] conclude that the centers of the polygons are slightly higher than the edges. It is noteworthy that these polygons are quite morphologically distinct from polygons found elsewhere on Mars that are interpreted to be caused by ice and/or water [e.g., *Rossbacher and Judson*, 1981; *Seibert and Kargel*, 2001]. The polygons on the lava flows are far more regular and are generally smaller than the ones interpreted to be related to water. In addition, the polygons formed by ice usually have raised edges.

[15] One of the most striking features on the surface of the Martian flood lavas are long grooves in the flow surface (Figure 6). These grooves are usually 1–10 km long and are parallel to the flow direction. There is often a topographic high or a collection of pressure ridges at the upflow end of a groove. These features are interpreted to be wakes cut into the flow top that form as the lava crust moves past a stationary obstacle [*Keszthelyi et al.*, 2000]. The fact that parallel grooves can be found across an area extending tens of kilometers across flow suggests that sections of crust on this scale moved in concert.

[16] The margins of the platy-ridged flows often transition to a surface that has distinct 10-m scale inflation features such as tumuli, inflation pits, and inflation plateaus [*Keszthelyi et al.*, 2000; *Lanagan and McEwen*, 2004] (Figures 6 and 7). The inflated margin of the flow is typically 100–500 m wide. However, in some cases the ridged surface extends to the very margin of the flow (Figure 5). The margins of the flow are very convoluted, showing a strong influence of small topographic obstacles. This suggests that the advancing front of the lava flow was quite thin and fluid. It is inconsistent with a high viscosity lava with evolved composition, such as an andesite.

[17] The lava also shows the ability to enter impact craters via quite narrow topographic breaches. In Figure 7 the lava can be seen filling a ~50 km wide crater by passing through a ~2 km wide passage. The presence of plates >2 km wide immediately inside the entry into the crater indicates that the plates formed within the crater, rather than being transported into the crater from outside. This image also shows that ridges can form on the plates with ≤1 kilometer of translation of the crust. This is an interesting contrast to the area shown in Figure 6 where a section of lava crust tens of kilometers in width moved as a coherent unit for >10 kilometers.

[18] Currently the MOLA topographic map is the best tool for tracing the extent of the young Martian flood lavas (though THEMIS images are rapidly nearing near global coverage as well). The flows that can be seen emanating from the ridges and shield near the Cerberus Fossae are generally several tens to a few hundred kilometers in length (Figure 3e). In contrast, some of the flows that pass through Marte Vallis into Amazonis Planitia (Figure 3f) are at least 1500 km long and probably >2000 km long. This is significantly longer than the longest mapped terrestrial flood basalt lava flow (the 760-km-long Pomona Member of the Columbia River Basalt Group, Washington, USA [Tolan et al., 1989]). The lobes we have identified are
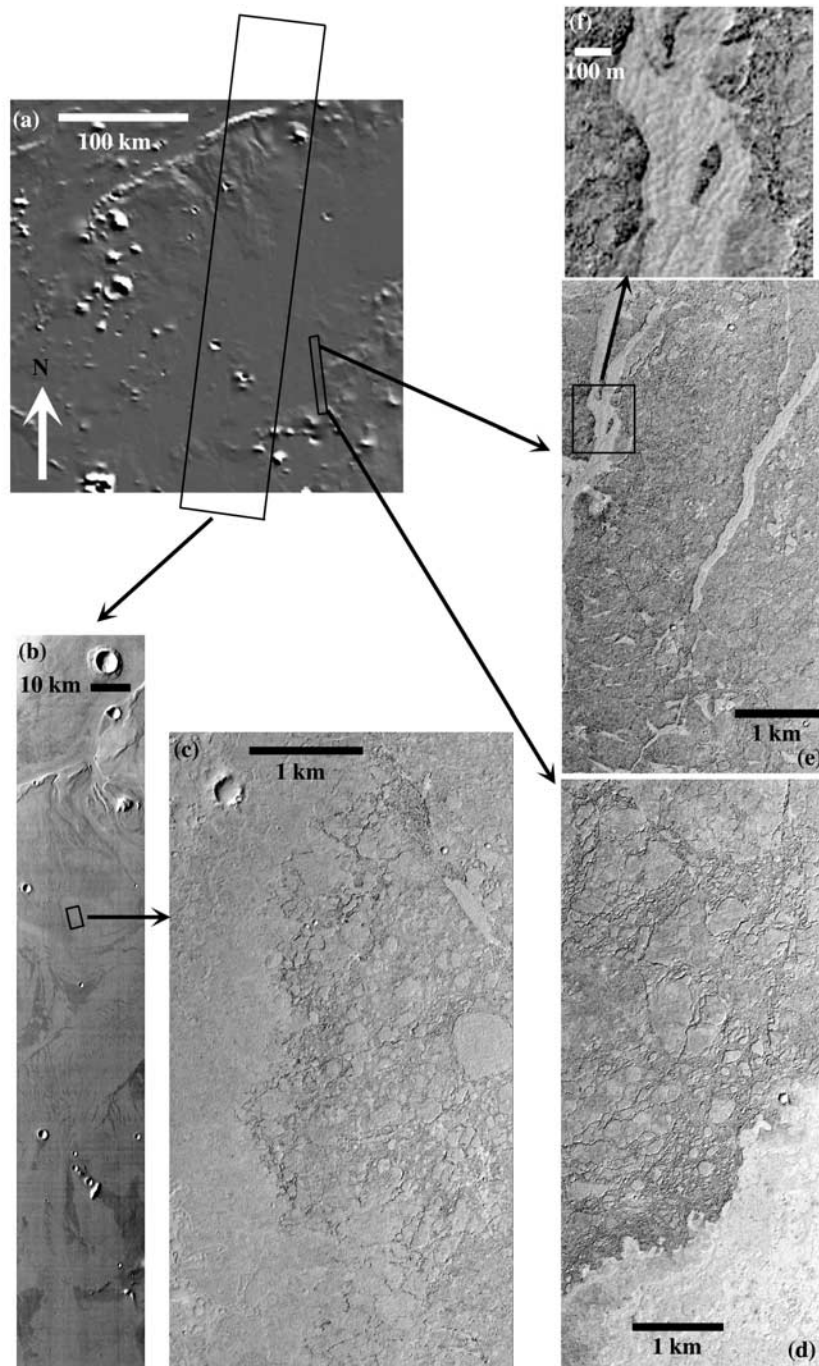

Figure 5

generally 100 ± 50 km wide. Thus, the typical volume for one of the Cerberus flood lava flows is between several hundred to a few thousand cubic kilometers. This is similar to typical terrestrial flood basalt units [*Tolan et al.*, 1989]. However, terrestrial flood basalt units are commonly "compound flow fields" and are composed of multiple flows and lobes [e.g., *Self et al.*, 1997; *Thordarson and Self*, 1998]. It is likely that individual Martian flood lava eruptions also produced multiple flows so it is plausible that the Cerberus flow fields involve $\sim 10^4$ km^3 of lava. *Lanagan and McEwen* [2004] estimate that the volume of the most recent flood lavas in the Cerberus plains cover $\sim 10^6$ km^2 and have a volume of $\sim 10^4$–10^5 km^3. This probably represents the products of a small number of eruptions.

2.3. Preliminary Emplacement Model

[19] *Keszthelyi et al.* [2000] presented a preliminary model for the emplacement of the platy-ridged flood lavas. This model was based on earlier examination of terrestrial analogs. While there are some examples of flows with platy-ridged morphology in Hawaii [*Takahashi and Griggs*, 1987; *Keszthelyi et al.*, 2000] and the Snake River Plain [*Greeley and King*, 1977; *Chapman*, 1999], features on a scale similar to the Martian flood lavas were only found in Iceland [*Keszthelyi et al.*, 2000]. The qualitative emplacement model involved the steady advance of an inflating pahoehoe sheet flow punctuated by surges in the lava flux that rafted away large sections of the upper crust. This was sufficient to explain the plates, pressure ridges between the plates, and wakes cut into the flow top. However,

it did not address the formation of larger ridges or the polygonal smooth surfaces.

[20] The more quantitative models presented by *Keszthelyi et al.* [2000] were only intended to provide very broad constraints on the conditions under which the Martian flood lavas formed. At the time, our understanding of how these lavas were emplaced was inadequate to produce a quantitative model of the emplacement of any individual Martian flood lava flow. However, the initial modeling was able to show that lava viscosities needed to be in the range of 100–1000 Pa s. Less viscous lavas would become turbulent and should not have produced flows tens of kilometers wide moving in concert. More viscous lava flows only a few tens of meters thick could not extend >1000 km over these shallow slopes without freezing. For the $\sim$100 Pa s lavas, flow velocities under an insulating crust a few meters thick needed to be greater than 0.2–0.8 m/s to avoid freezing after 1000 km of flow. This suggested sustained lava flux >10^4 m^3/s and eruption durations of a few years.

[21] Modeling of the flows during surges was based on thermal models for aa flows [*Crisp and Baloga*, 1994; *Keszthelyi and Self*, 1998]. While these initial efforts were greatly hampered by a lack of understanding of how the disrupted crust might behave, a few robust conclusions could be made. To avoid freezing during even a few kilometers of transport, the crust had to be mixing with the interior of the flow at a rate slower than very vigorous Hawaiian aa flows. As the presence of large plates suggested, the top of the flow would have been stable on the timescale that the flow

Figure 5. Detailed morphology of surface of the most pristine Martian flood lavas, south of Athabasca Valles. (a) MOLA topographic context, same as Figure 3c. The topographic rise cutting diagonally across the region is a tectonic wrinkle ridge that kept most of the floodwaters to the northwest. However, there are several prominent locations where the ridge was breached and some water flowed to the southeast. While some minor deposition of flood-carried sediments probably occurred, the morphology of the lavas appears unaffected at the 10–100 m scale. (b) The 100 m/pixel THEMIS daytime thermal infrared image I0329009. While some flood-carved features can be seen north of the wrinkle ridge, the streamlined temperature patterns in the surface to the south of the ridge are related to the surface morphology of the young flood lavas. In particular, areas that are cooler correspond to regions between rafted plates of lava crust. (c) The 3.5 m/pixel MOC image M2202268 showing typical "platy-ridged" morphology that is common on Martian flood lavas. The plates appear to be 100–1000 m scale pieces of coherent lava crust that have been rafted a short distance on top of the moving liquid crust beneath. The ridges appear to be formed by pushing together parts of the crust that have failed in compression (i.e., are "pressure ridges"). (d) Southern portion of 4.41 m/pixel MOC image FHA01372 showing the margin of a platy-ridged lava flow. In this case, the platy-ridged texture extends to the very margin of the flow. In many other cases, the lava transitions to inflated pahoehoe at the margin. (e) Northern portion of MOC image FHA01372 showing a platy-ridged surface that has undergone a second episode of tearing of the crust. The coherent plates in this case are kilometers in scale and have a surface of smaller plates and ridges. The region between the larger plates has a characteristic "polygonal" texture. (f) Close-up of polygonal texture. The polygons are typically of order 10 m in scale and are slightly raised in the center.
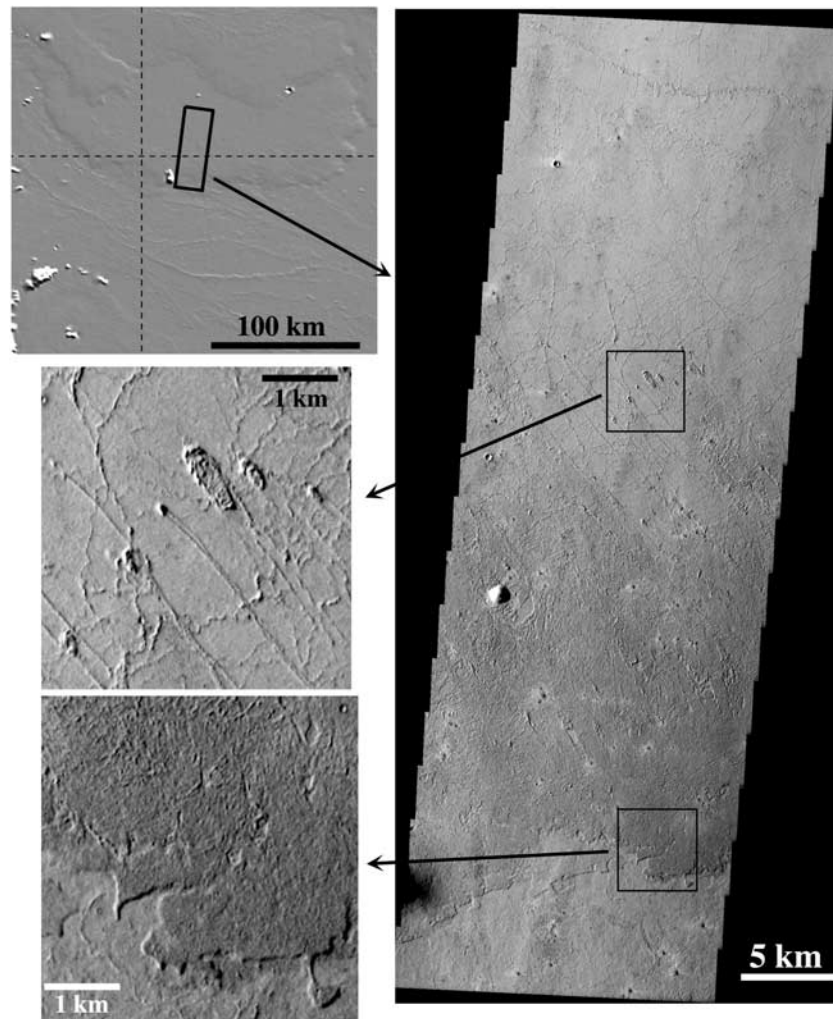
Figure 6. Detailed geomorphology of the margins of a >350 km long flow lobe in the Cerberus plains. Top left is a context map using MOLA topography. This is the same region as Figure 3e. On the right is the 18 m/pixel THEMIS visible image V05262021. The flow morphology transitions from a relatively smooth surface with large plates and few pressure ridges near the center of the lobe to a surface dominated by ridges toward the margin. However, the outermost kilometer or so of the flow has a very smooth surface. On the center left is a blow-up of one of the most striking features of these flood lavas: wakes kilometers long cut into the surface of the flow. These appear to form when the moving crust is torn as it is pushed past a stationary obstacle that protrudes through the flow. If the obstacle is large, the crust piles up in front of the obstacle. However, in the case of narrow obstacles, the crust is pushed up on either side of the obstacle and then rafted along on the undisrupted crust. The bottom left shows a blow-up of the morphology of the flow margin. In this case, the margin is characterized by a smooth surface that appears to have a very uniform height. This is consistent with an inflated surface, but this image lacks the resolution to identify surface features that are diagnostic of inflation. Features diagnostic of inflation are seen in MOC images of other lobe margins [*Keszthelyi et al.*, 2000; *Lanagan and McEwen*, 2004].

moved a few kilometers (i.e., greater than a few minutes). Lava flux during the surges was estimated to be of order 10^5–10^6 m³/s.

[22] The primary goal of our fieldwork in Iceland was to gain a better understanding of how platy-ridged lava flows are emplaced so we could improve on the initial models of *Keszthelyi et al.* [2000].

3. The 1783–1784 Laki Flow Field

[23] *Keszthelyi et al.* [2000] found that portions of the 1783–1784 Laki Flow Field appeared very
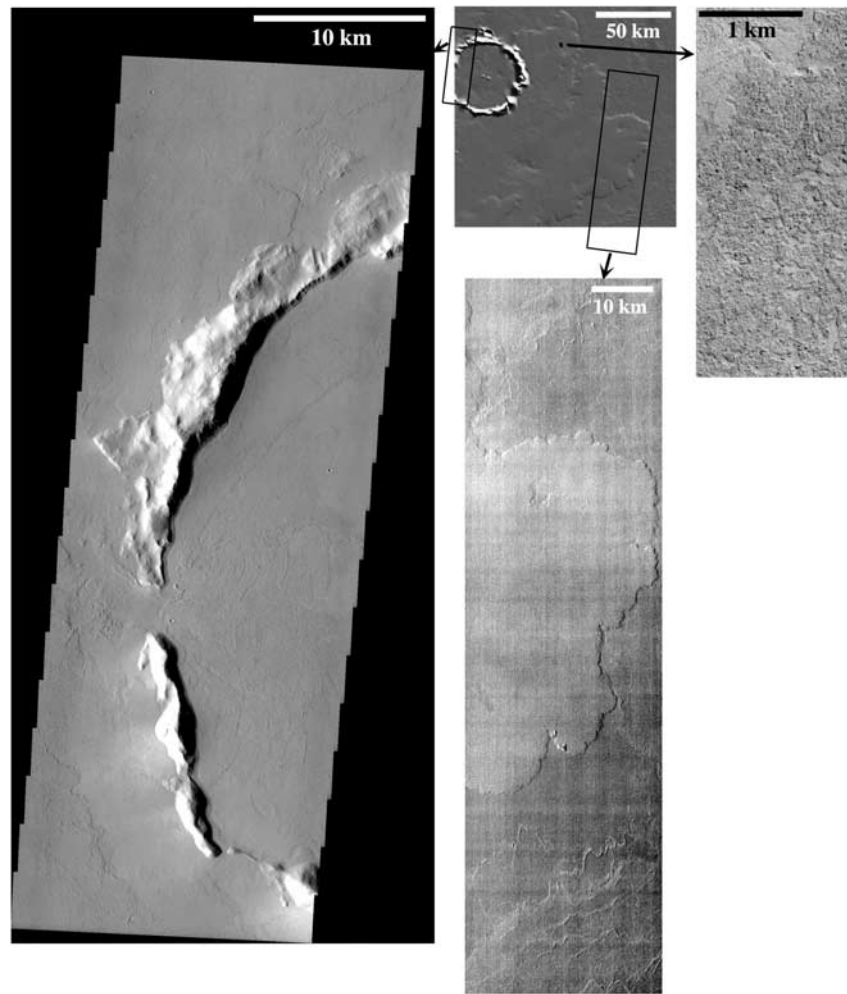
Figure 7. Detailed geomorphology of the distal end of >1500 km long flow lobes. Top center: MOLA topographic context map of the region (same as Figure 3f) showing the terminus of lavas that started from the Cerberus plains, flowed through Marte Vallis, and ended in western Amazonis Planitia. On the left is THEMIS VIS image V02440003 at 18 m/pixel. Note the presence of plates with ridged surfaces within the crater. Some of the plates are larger than the breach in the crater rim, indicating that the plates formed within the crater (as opposed to carried into the crater). The bottom center shows THEMIS daytime infrared image I04250002 at 100 m/pixel. Note that the flow with the prominent crenulated margin lies on top of a well-preserved platy-ridged lava flow. The overlying flow has a smooth surface at 100 m/pixel. On the right is MOC image M1400230 at 3.02 m/pixel. This image shows that the surface that looks smooth at 100 m/pixel actually is composed of a complex, hummocky texture at higher resolution. Some of this hummocky texture is similar to inflated pahoehoe surfaces on Earth.

similar to the Martian flood lavas in images acquired at similar resolutions. The Laki Flow Field has been carefully studied in the past, including excellent written records by eyewitnesses to the eruption [e.g., *Steingrímsson*, 1998]. However, the "platy-ridged" morphology of the lava had not been documented in the scientific literature beforehand. Thus we have initiated a program of fieldwork on the lavas to better understand the formation of the specific features that are common with the Martian flood lavas. In this section, we document the results of

our initial fieldwork. However, first, we provide a concise synopsis of the 1783–1784 eruption and the flow field it produced.

3.1. General Description

[24] The eruption started on June 8, 1783 and lasted 8 months, ending on February 7, 1784. It produced the largest basaltic eruption with good written eyewitness records. The eruption is most famous for killing about 20% of Iceland's population. This was the result of acidic volcanic gases
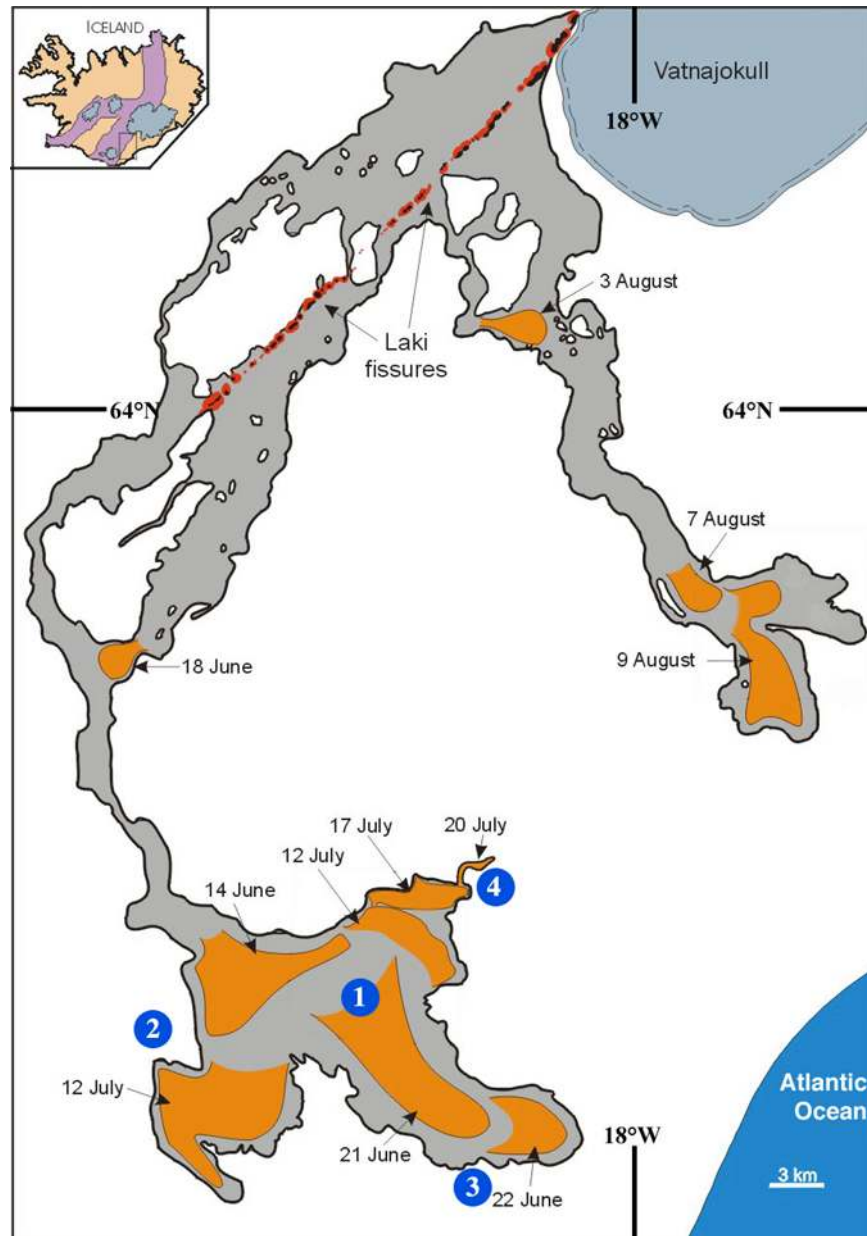
Figure 8. Map of the Laki Flow Field, Iceland. Locations of the active flow front on different dates of 1783 are shown. Localities described in detail in section 3.2 are marked with blue circles. Note the Laki fissures (Lakagigar) extending out from under the Vatnajokull glacier.

killing the nation's livestock, leading to a catastrophic famine. Along with ∼250 Mt of volcanic aerosols, the eruption produced ∼15 km^3 (dense rock equivalent) of lava. Basaltic ash covered ∼7.5 × 10^5 km^2 and lava flows buried almost 600 km^2 with flows that reached as far as 66 km from the vent [*Thordarson and Self*, 1993; *Thordarson et al.*, 1996] (Figure 8).

[25] The vents consist of a series of cinder and spatter cones following a 27 km long fissure system (Figure 9). The fissure can be divided

into 10 distinct segments. These generally opened from west to east, with most segments feeding a single episode of the eruption. However, during Episode 5, five different fissure segments were all active. A total of 11 different eruptive episodes from the fissures can be discerned from the written records and investigation of the near-vent deposits [*Thordarson and Self*, 1993].

[26] The eruption rates were highly variable during the 8 months of the eruption. In general, the

Figure 9. Photo of Lakagigar (the vents for the Laki flow field). Fissure system is 27 kilometers long. Note that all the spatter cones along the fissure lie inside the graben that formed during the eruption (normal faults marked with arrows). If the graben were to open further, all the vent structures could be obliterated. Such a process may explain the dearth of visible vent features associated with the Martian flood lavas.

eruption rates decreased during the eruption. The first few days appear to have reached $>10^4$ m³/s, peaking at $\sim 2 \times 10^4$ m³/s [*Thorarinsson*, 1968; *Thordarson and Self*, 1993]. By the end of the eruption, rates had dropped to 80–200 m³/s. Mean eruption rates for each episode decreased from ~ 8000 m³/s for episodes 1–3 to ~ 2000 m³/s for episodes 7–10. The lavas are tholeiitic basalts, with compositions of the bulk lavas and glassy margins given in Table 2.

[27] The Laki lava flows passed through the highlands surrounding the vents via two river gorges and out onto a broad coastal plain (Figure 8). During the latter part of the eruption, lavas came down the eastern Hverfisfljot River Gorge and mostly formed classic inflated pahoehoe. We focused on the earlier, western, flows that traveled along the Skaftá River. On the coastal plains below the Skaftá River Gorge, the Laki lavas exhibit all the morphologic features seen in Martian platy-

ridged lava flows. We know that this region was first covered between mid-June and mid-July, 1783. The bulk of the features of interest are in an area covered on June 21, 1783 (Figure 8).

[28] We have tried to estimate the physical properties of the lava in this area. The MELTS program [*Ghiorso and Sack*, 1995; *Asimow and Ghiorso*, 1998; *Ghiorso et al.*, 2002] was used to calculate the liquidus temperature, lava temperature, and predicted crystallinity of the distal lavas of interest (Table 3). While the liquidus temperature for the Laki lavas is quite high, the actual erupted and flowing lavas seem to have had temperatures very similar to recent active Hawaiian flows [e.g., *Keszthelyi and Denlinger*, 1996].

[29] We use the MAGMA program of Ken Wohletz to calculate both the bulk density of the lava and the viscosity of the liquid portion of the lava. The viscosity is calculated using the technique of *Bottinga and Weill* [1972]. Correcting the viscosity for the solid and gas phases within the lava is difficult. With 38 vol.% crystals and 20–30 vol.% vesicles, the effects of these phases are very significant. Field experience in Hawaii suggests that at very low strain rates (i.e., low applied stress), bubbles can act as rigid spheres, stiffening the lava. However, at high strain rates (or high applied stress) bubbles weaken the lava [*Keszthelyi and Self*, 1998]. In Table 3, we treat bubbles as rigid spheres and use the technique presented by *Pinkerton and Stevenson* [1992] to estimate the bulk viscosity of the lava. The combination of vesicles and crystals can exceed the limits of this technique, suggesting that at low applied stresses the lava is a stiff foam with infinite viscosity. We therefore suggest that the bulk viscosity of the Laki

Table 2. Major Element Analyses of Some Laki Lavas[a]

Lava Type	Strombolian Tephra	Proximal Flow (Whole Rock)	Distal Flow (Whole Rock)	Distal Glass
SiO_2	49.91	49.68	49.56	49.78
TiO_2	3.04	2.70	2.65	3.80
Al_2O_3	13.19	13.93	13.97	11.85
FeO	14.16	13.39	13.38	16.17
MnO	0.21	0.21	0.22	0.27
MgO	5.42	5.56	5.75	4.69
CaO	9.84	10.35	10.38	9.43
Na_2O	2.76	2.58	2.73	2.66
K_2O	0.45	0.41	0.40	0.55
P_2O_5	0.30	0.30	0.31	0.36

[a] Data from *Thordarson* [1995]. The distal glass provides an estimate of the composition of the liquid component of the lava far from vent. The sample with the glass contained 38 vol.% crystals.

Table 3. Estimated Properties of the Distal End of the Laki Lava Flows[a]

	Liquidus	Estimate From Glass Composition	Estimate From Model Crystallization of Bulk Rock
Temperature, °C	1180	1133	1118
Crystallinity, vol.%	0	23	38
Liquid density, kg/m³	2990	3050	3010
Bulk density, kg/m³	2250	2390	2420
Liquid viscosity, Pa s	22	39	47
Solid + liquid, Pa s	22	130	580
With 25% vesicles, Pa s	250	2200	∞

[a] Properties calculated using the java MELTS program (http://ctserver.uchicago.edu/), the MAGMA program (http://www.ees1.lanl.gov/Wohletz/Magma.htm), and compositions listed in Table 2. Calculations assume that oxygen fugacity is fixed at the QFM buffer and that the liquid is saturated with water (i.e., water content ~0.03 wt.%). Liquid viscosity calculated using the method of *Bottinga and Weill* [1972]. Correction for crystals and vesicles use the Einstein-Roscoe equation [*Pinkerton and Stevenson*, 1992]. For vesicles, this is appropriate only for low strain rates and short timescales.

lava in the area of interest varied between 100 Pa s and essentially infinity, depending on the local strain rate. Lava also exhibits visco-elastic properties in the field [e.g., *Hon et al.*, 1994], so the effective viscosity is also a function of the timescale of interest. The infinite viscosity of the stiff foam only applies on timescales of seconds to perhaps minutes. On longer timescales, the bubbles and crystals can move within the melt, breaking down the foam. This expectation of highly variable viscosity of the lava has profound implications for the motion and modeling of these lavas. We will show field evidence that supports the suggestion that portions of the Laki lava exhibited both highly viscous and relatively fluid behavior during emplacement.

3.2. Detailed Morphology of Platy-Ridged Facies

[30] As noted earlier, we concentrated our field examination to the portion of the Laki Flow Field that exhibits a platy-ridged surface morphology. This is the area where the western arm of the Laki Flow Field spread across the coastal plains. The surface that the Laki lavas moved across included both fluvial sediments and earlier lava flows (of which the 938 AD Elgjá Flow Field is the most extensive). It is important to note some constraints on our field observations. Examination of the surface is hampered by a layer of moss that is generally 10–50 cm thick. However, this moss could be easily stripped by hand and a few areas

have only a thin veneer of moss. Cross-sections into the lava are limited to a few cuts provided by rivers and roads. Almost all of these cuts are only a few meters deep, insufficient to penetrate the crust of the flow, much less provide a complete cross-section.

[31] The bulk of the lava surface in this area consists of large topographic ridges oriented perpendicular to the direction the lava flowed. However, the most distal few hundred meters of the lava commonly has an inflated pahoehoe surface. The ridges are generally 5–15 m tall, ~40 m wide, and ~200 m in length. The ridges are commonly closely packed, leaving no flat (or concave upward) surface in between them. As mentioned earlier, there are a number of grooves cut into the ridged surface and there are plates with ridged and with smooth surfaces.

[32] After extensive examination of many localities within the platy-ridged portion of the Laki Flow Field, we have selected four locations from which to provide detailed observations. These areas are labeled in Figure 8. The first locality provides the best description of the majority of this region of the Laki Flow Field. It is unique only in the excellent quality of the expression of the main morphologic features of platy-ridged lava in a relatively small area. Localities 2 and 3 provide cross sections into the top of the flow and locality 4 demonstrates some interesting differences from the bulk of the flow field.

3.2.1. Locality 1

[33] The area labeled "1" in Figure 8 contains all the morphologic features we associate with the Martian flood lavas: ridges, plates, and grooves (Figure 10a). The groove we examined is one of the most prominent examples on the entire Laki Flow Field. It is 4 m deep with a ~1 m tall levee on each side. Both the groove and the levees are about 20 m wide (Figure 10b). The groove can be traced for about 1.5 km and curves parallel to other grooves in the area. The prominent mound at the front of the groove is 14 m tall and about 80 m in diameter.

[34] The mound, the levees, and the surrounding lava all consist of breccia. Figure 10c shows an almost moss-free portion of the breccia. The breccia consists of blocks ~1 m in diameter that in turn consist of 10–20 cm clasts. The smaller clasts are interlocked and sometimes weakly welded together to form the larger blocks. Loose centimeter-scale
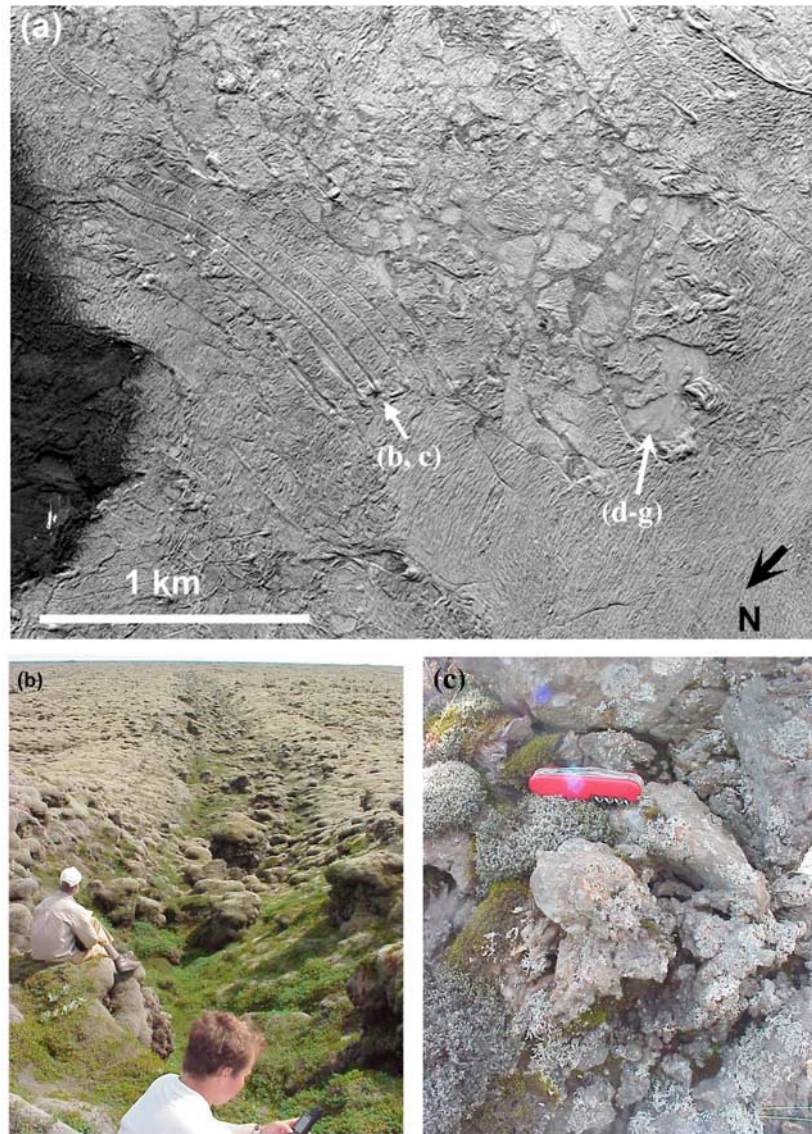
Figure 10. Photos of the Laki Flow Field at location marked "1" in Figure 8. (a) Aerial photo. Note the 100 m scale plates, ridges, and grooves. Locations of Figures 10b–10g are marked with white arrows. (b) Photo of large groove cut in the crust of the Laki lava flow. Photo taken from mound of brecciated material at the front of the groove. The mound was 14 m tall and had an average slope of ∼15°. The groove is about 4 m deep. The floor has a smooth surface, similar to that seen in Figures 10d–10g. We interpret this feature to have formed as the lava crust moved past a stationary obstacle in the flow, with the groove forming in the wake of the obstacle. (c) Close-up photo of breccia making up the mound at the front of the groove. Note the mix of moderately vesicular and dense lava and the convoluted shapes of the clasts. (d) View of margin of "ridged" lava and "smooth" lava with 10-m-scale polygons. Note the sharp contact with minimal collapse of the brecciated ridged material onto the smooth area. (e) Close-up of the smooth lava with people for scale. Note the undulating surface of the polygonally fractured lava. The edges of the polygons are topographically low, as in the polygonal surfaces in the Cerberus plains of Mars. (f) Excavation of the moss to expose the surface of the smooth lava. Note the flat, pahoehoe, surface. (g) Close-up of the excavated lava surface. Note the large stretched vesicles characteristic of pahoehoe. The spinose nature of the surface suggests that this was relatively viscous lava (compared to typical Hawaiian pahoehoe).

fragments generally fill the space between the meter-scale blocks. The lava that makes up the smaller clasts has variable characteristics. The most common examples contain ∼15 vol.% irregular, subrounded, 1–10 mm diameter vesicles. Other clasts are dense massive aphanitic basalt. The vesicular clasts commonly have highly irregular, contorted shapes while the dense clasts more often
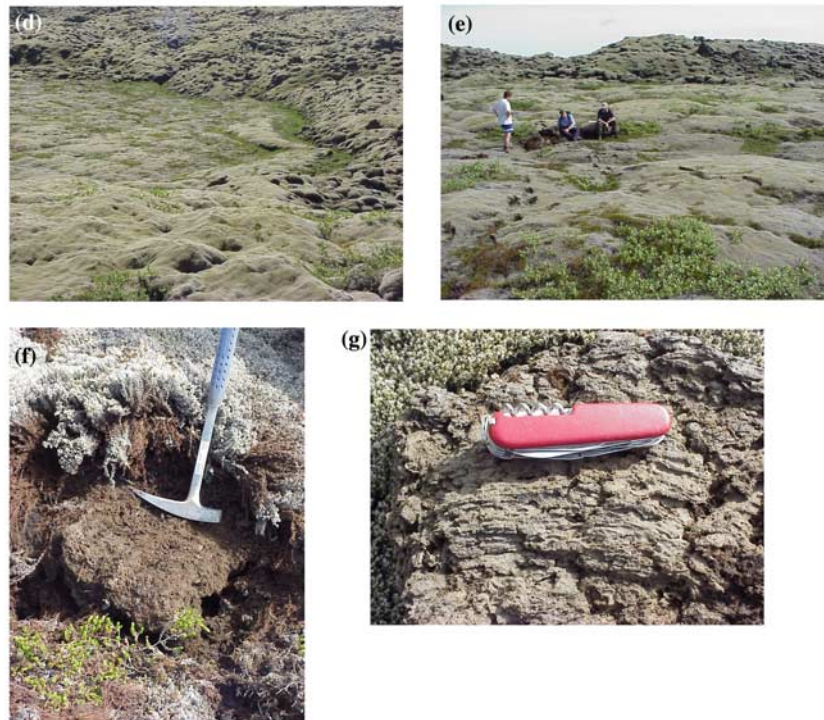
Figure 10. (continued)

have simpler but angular shapes. The surfaces of the vesicular clasts rarely have aa-like spinose textures. Instead, they more commonly have a largely glassy surface with stretched vesicles that characterizes pahoehoe lavas.

[35] The first order interpretation of this breccia is that it must have formed while the clasts were hot and the top of the lava flow was in motion. The contorted shapes of many of the clasts require plastic deformation. The occasional welding between clasts indicates that some of the breccia was near its solidus temperature during brecciation. The presence of blocks of breccia within the breccia does not allow for a single, discrete brecciation event. Instead, it suggests, but does not definitively prove, that there were at least two episodes of brecciation. The generally low vesicularity of the clasts suggests that much of the lava involved was degassed. The presence of pahoehoe-like surfaces on many of the vesicular clasts suggests that strain rates were low within the breccia and/or the lava in the clasts was quite fluid [*Peterson and Tilling*, 1980]. Given the relatively high viscosities we predict for these distal lavas (Table 3), we conclude that the strain rates were low.

[36] We also examined the smooth area between the ridged plates (labeled d-g in Figure 10a).

Figure 10d provides an overview of the contact between the ridged plates and this smooth area. This photo was taken from the ∼25 m tall mound of breccia immediately upflow from the smooth area. The contact is sharp, with only a few pieces of breccia having fallen onto the lower smooth area. Figure 10e provides a slightly closer view of the undulating surface of the smooth area. Note the even depths of the footprints in the ∼10-cm thick moss cover. The even thickness of the moss means that the undulating nature of the surface here is an accurate representation of the 10-cm scale topography of the underlying lava. The lava surface consists of upwarped regions, ∼10 m in diameter, with polygonal margins. Where the moss cover was removed, the lava consists of flat slabs (Figure 10f). The slabs are 3–5 cm thick and contain 25–30 vol.% well-rounded, 1–9 mm diameter vesicles. These slabs have classic pahoehoe surfaces with long stretched vesicles (Figure 10g). The lower surfaces of the slabs have drips and glazing indicative of separation at the interface between solid and liquid lava.

[37] The surface in this smooth area is identical to that found on Hawaiian lava lakes [e.g., *Swanson*, 1973]. Therefore we interpret these areas as having formed under very quiescent conditions. From the

spatial arrangement of the plates, mounds, and smooth areas, we infer that the smooth material welled into tears in the brecciated crust. As such, we believe that this provides a sample of the liquid lava flowing within the lava flow at the time that the brecciated crust was disrupted. The lava lake-like nature of the surface indicates that the disruption of the crust was a relatively gentle affair.

3.2.2. Locality 2

[38] This location (labeled "2" in Figure 8) is one of the deepest cuts into the brecciated flow top breccia of the Laki Flow Field. The cut is provided by the Eldvátn River. Figure 11a provides an overview of the outcrop, which is just south of the Eldvátn Bridge. Figure 11b provides a closer view of the cut. Note the tape measure laid across the outcrop with 1 m of tape rolled out. The layer of breccia varies between 4–5 m thick with a poorly exposed contact with the underlying dense interior of the flow. While a few larger blocks and plates are present, the breccia here is dominated by ~10 cm diameter irregular clasts. There is also about 10 vol.% void space and 15 vol.% sub-centimeter clast fragments in the breccia. The clasts are not tightly interlocked or welded, so it is possible to examine individual clasts in more detail than at locality 1.

[39] There is a remarkable variety of clast types (Figures 11c–11f). There are occasional ~10 cm thick plates of lava with pahoehoe ropes on one surface and frozen drips of lava on the opposite side. We also found one $20 \times 10 \times 5$ cm clast with the spinose surface characteristic of aa lava. However, the bulk of the clasts have subrounded, contorted shapes with fragments of pahoehoe-like surfaces. Vesicularity ranges between 5 and 50 vol.%, vesicle sizes range from 0.2 mm– 1.5 cm, and vesicle number density varies between 6–20 vesicles/cm². Some clasts show scrape marks where they were dragged past a solid surface while in a plastic state (Figure 11d). There are also clasts that are wrapped around other clasts (Figure 11f).

[40] Another key observation at this outcrop was the presence of a "blade" of dense lava protruding from the interior of the flow into the breccia. This blade is >40 cm tall, ~15 cm wide, and appears to extend several meters in length. It has small branches a few centimeters in scale. The margins of the dense lava are fragmented into mm-scale particles, apparently due to sudden thermal contraction and mechanical abrasion of the blade when it was emplaced. We conclude that this is an intrusion of material from the interior of the flow into the breccia.

[41] Overall, these observations provide further evidence that the breccia must have formed while parts of the lava flow were mobile and plastic. It also suggests that the brecciation has mixed lava from different facies within the flow; some clasts are typical of the flow top, while others have features typical of the core of a flow. The paucity of spinose aa again suggests that strain rates were generally quite low during the brecciation process. The aa clast may represent an unusually viscous piece of lava that was torn at low strain rates or may record a short-lived, localized, high strain rate event.

3.2.3. Locality 3

[42] The point labeled "3" in Figure 8 corresponds to another Eldvátn River cut. This cross-section is near the distal margin of the Laki Flow Field. The cut again penetrates a flow top breccia with the most common clasts being contorted pieces of lava 10–20 cm in diameter. What is unique at this location is the presence of intact meter-scale pahoehoe lobes and multimeter pieces of inflated pahoehoe.

[43] The pahoehoe lobes (colored purple in Figure 12c) have an outer margin that is deformed around the breccia clasts. The lobes have 7–10 cm scale ropes on their surface. The radial cooling fractures are reminiscent of the fractures in pillow basalts and require rapid cooling from all sides. The vertical/radial distribution of vesicles within the lobes is similar to that seen in classic pahoehoe lobes: 20–30 vol.%, 0.2–20 mm, coalesced vesicles at the surface; vesicularity diminishing ~5 vol.% every 10 cm inward and maximum vesicle size dropping to ~1 mm; and large (6– 10 cm) elongated vesicles in the center. We conclude that these lobes record the intrusion of relatively fluid and vesicular lava into an existing breccia.

[44] Other coherent sections of the lava contain clefts and fractures typical of inflated pahoehoe (colored green in Figure 12c). These intact areas are 3–4 meters in scale and are close to being upright. The cleft surfaces have bands of vesicles that are common in inflating lavas [e.g., *Cashman and Kauahikaua*, 1997]. The original lava surface that is preserved in other intact areas has classic pahoehoe ropes.

[45] This outcrop appears to cut through the transition between the brecciated lava and the inflated
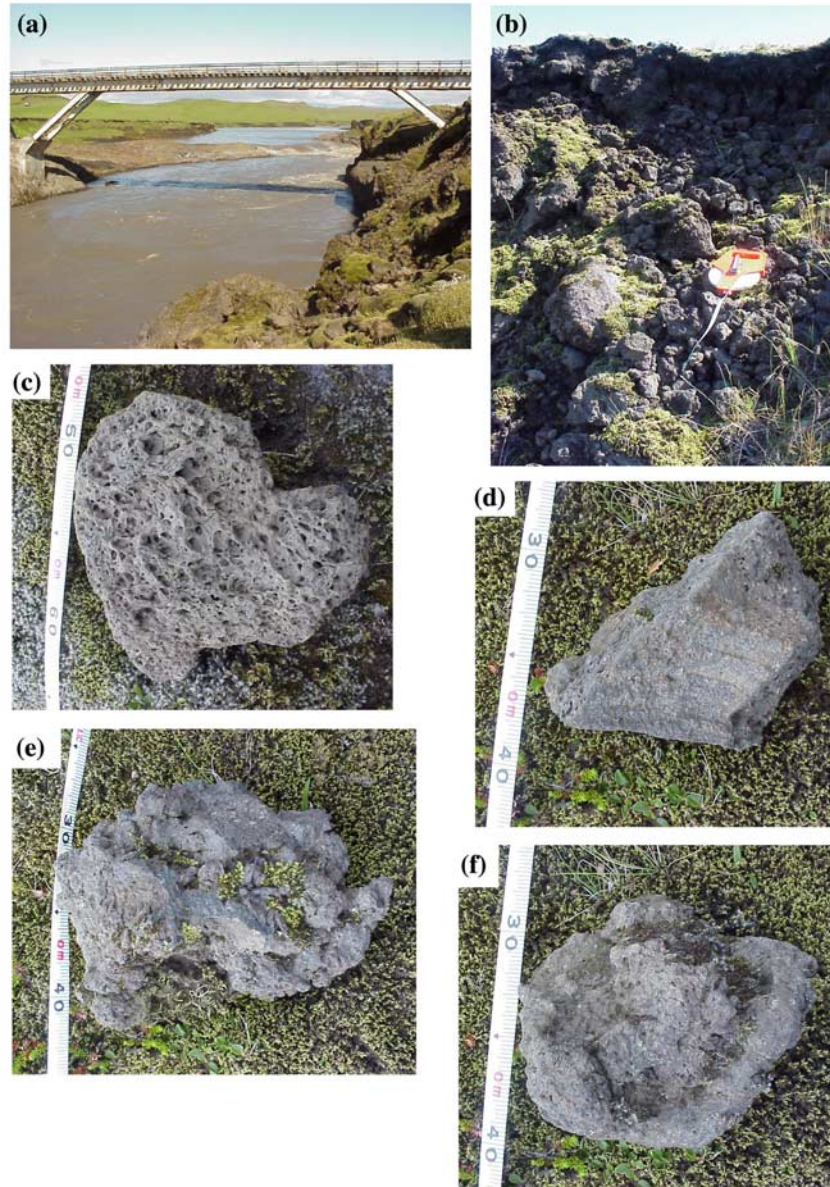
Figure 11. Photos of flow top breccia at location 2 in Figure 8. (a) Overview of outcrop provided by the Kúdafljót River. Outcrop is on the southeast (right-hand) bank of the river. (b) Exposure of the brecciated flow top. Total thickness of breccia is 4−5 m. Breccia in this location is clast supported and generally not agglutinated or welded. (c) Close-up of a breccia clast composed of a slab of vesicular pahoehoe. Slab is ∼10 cm thick and appears to have had its edges rounded, probably by mechanical abrasion by motion within the breccia. (d) Groove-like marks on another broken slab in the breccia. These marks are interpreted to have formed when another clast scraped against this clast while this (bottom) side of the slab was still hot and plastic. (e) Typical clast in the breccia with convoluted margins and a surface with stretched vesicles characteristic of pahoehoe. The convoluted shape of the clast seems to have been the result of twisting and folding a hot, still plastic, piece of lava. (f) Clast wrapped around and welded to another clast. The folded, outer clast is chilled against the inner clast. Clasts such as this one provide the best evidence that the flow top breccia included a mix of hot and cold pieces of lava.

pahoehoe margin of the flow. The spatial relations between the sections of inflated pahoehoe and the breccia require that the inflated pahoehoe formed first. The breccia is pushed into the inflated pahoe-hoe flow, gently pushing apart 3−4 meter segments of the older lava. The pahoehoe lobes are then intruded into the breccia, presumably from the fluid interior of the flow. There is little, if any,
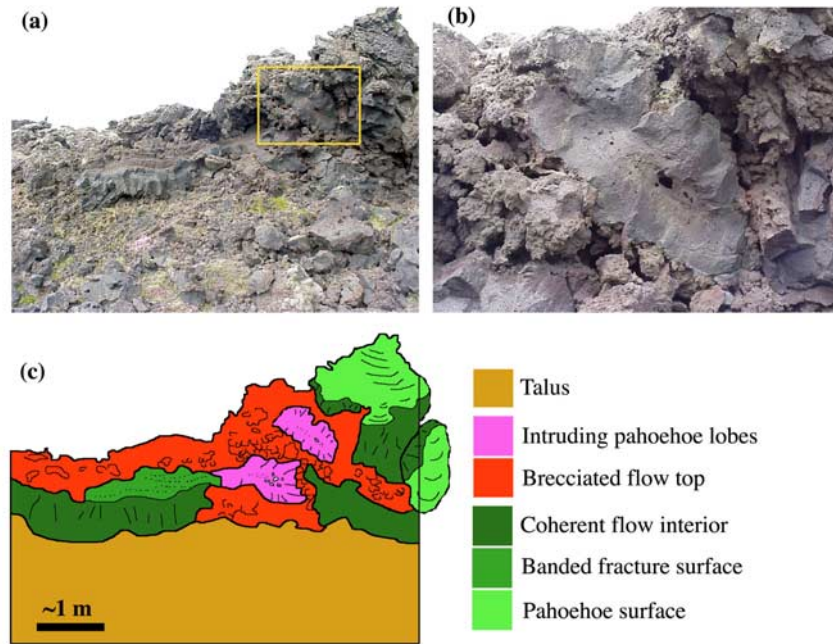
Figure 12. Photo of pahoehoe lobes in flow top breccia at location 3 in Figure 8. (a) Overview of outcrop cut by Eldvátn River in the distal end of the Laki flow field. Yellow box shows the location of the close-up. (b) Close-up of a pahoehoe lobe intruding the flow top breccia. The lobe is about 1 m long and 0.55 m tall. The top has 7–10 cm wavelength ropes and a classic pahoehoe surface. The interior of the lobe has a radial fracture pattern, indicating cooling from all sides. The vesicles are elongated along the long axis of the lobe, suggesting moderately viscous lava. The bottom of the lobe conforms to the shape of the breccia, indicating that the lobe was emplaced after the breccia had formed. (c) Outcrop sketch at the same scale as Figure 12a. Legend has the older materials toward the bottom. Areas drawn in green are coherent lavas with characteristics of inflated pahoehoe lobes such as a banded fracture surface that appears to be the wall of an inflation cleft. The breccia appears to have pushed meter-scale pieces of pahoehoe crust outward. This flow top breccia is intruded by the pahoehoe lobes.

deformation after the emplacement of these pahoehoe lobes, because the lobes themselves are not disrupted.

3.2.4. Locality 4

[46] The point labeled "4" in Figure 8 is a small (~200 m wide, 2 kilometer long) sheet lobe that extended from the main Laki Flow Field down the Skaftá River on July 20, 1783. This lobe has a platy-ridged surface morphology and provides a different view of the processes that form this surface morphology. The margins of the lobe have classic inflation features including pits and clefts (Figure 13b). The depth of the inflation pits range from 3–8 meters and are10–20 m in diameter. The vertical distribution of vesicles is typical of inflated pahoehoe [e.g., *Cashman and Kauahikaua*, 1997; *Thordarson and Self*, 1998] with vesicularity grading from ~25 vol.% at the surface to ~15 vol.% a meter down, and cm-scale horizontal zones of higher vesicularity.

[47] The upper surface of the lava flow is composed of ridges of slab pahoehoe (flat slabs of lava with smooth pahoehoe surfaces on one side of the slab) and flat plates of smooth pahoehoe. Toward the margins of the flow, the slabs are only ~5 cm thick and 20–40 cm in lateral extent. In the center of the flow, the slabs are 14–16 cm thick and 40–300 cm in lateral extent. The transition between the surfaces with smaller and larger plates is marked by a sharp shear zone only a few centimeters wide. The spatial relations across the shear zone indicate that the interior of the flow moved further than the margins.

[48] The ridges are composed exclusively of slabs. There is no evidence of the contorted clasts, dense intrusions, or pahoehoe lobes seen at the other localities we described within the main Laki Flow Field. The thicker slabs have often arranged themselves at right angles to each other (Figures 13e and 13f). One result of this is that the void space in the ridges is often 50–70 vol.%. The slabs have

Figure 13. Photos of plates and pressure ridges at location 4 in Figure 8. (a) Overview of tongue of the Laki Flow Field that followed the Skaftá River valley. The lobe margins show classic inflation features, but the interior of the lobe has a series of 100-m-scale plates separated by pressure ridges. (b) Close-up of the plates and ridges. Note one-lane road for scale. (c) Surface of a plate with people for scale. Note gently undulating surface like in Figure 10e. (d) Contact between plate and ridge. Note that the undulations are convex upward, like the smooth surface in Figures 10a–10g. The contact between the ridge of breccia and the smooth plate is sharp. (e) Overview of a pressure ridge. Note that the breccia consists exclusively of slabs of pahoehoe ~1 m across and ~15 cm thick. (f) Close-up of pahoehoe slabs. The base of the slab has frozen drips of lava, indicating that the slab was in contact with liquid lava immediately before it was pushed up. The pressure ridges are typically >50% void space and contain many near 90° corners. This type of surface should appear exceptionally rough in radar images.

smooth pahoehoe surfaces on one side and frozen drips on the other, indicating that they formed by disruption of a pre-existing pahoehoe surface with liquid lava below.

[49] The smooth plates between the ridges have the same smooth pahoehoe surface that the slabs do (Figures 13c and 13d). The pahoehoe surface is divided into gently upwarped polygonal sections.

The sections are typically 4–7 m across and have centers raised ~10 cm relative to the margins. The vesicularity and crystal texture of the material in the smooth plates is identical to that of the slabs in the ridges.

[50] Our interpretation of the sequence of events that formed this lobe begins with the formation of a smooth pahoehoe surface. Then different
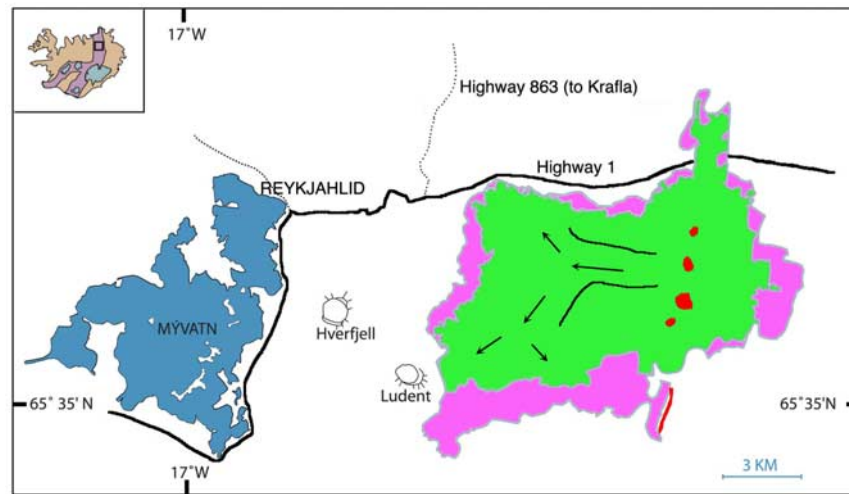
Figure 14. Location map of the Búrfells Lava Flow Field in north-central Iceland. There is another lava flow sometimes referred to as the Búrfells lava in southern Iceland. The example we examined is just east of the town of Reykjahlid (on the coast of Lake Myvatn) and just south of Krafla Volcano. The platy-ridged facies is shown in green, inflated pahoehoe is shown in purple, and vent constructs are shown in red. The margins of the sheet flow with a mobile crust and the direction of flow are shown in black.

parts of this surface were disrupted at different times. The thickness of the slabs provides an approximate measure of the time between emplacement of the liquid lava and the secondary disruption. We use the empirical cooling model of *Hon et al.* [1994] for this translation. Comparison of this empirical model with a relatively complex numerical cooling model [*Keszthelyi and Denlinger*, 1996] suggest that the crust growth rate of *Hon et al.* [1994] should be no more that 25% in error with changes in the lava properties and environmental conditions [*Self et al.*, 1998]. The 5-cm-thick slabs found near the margin of the flow were probably formed 20–30 minutes after the lava surface started to freeze. In contrast, the 15-cm-thick slabs in the center of the lobe were probably broken ~4 hours after the initial emplacement of the flow. While this might suggest two separate, spatially localized, episodes of disruption, it is more likely that this indicates that the age of the initial smooth surface varied by >3 hours across the ~200 m width of the lobe. The locations of the inflation pits suggest that significant inflation of the lobe took place after the disruption event(s) and the platy-ridged surface had cooled into a coherent upper crust. This sequence of events is quite different from what we infer to have taken place in locality 3.

[51] We will try to draw more general conclusions from the field observations after describing some additional examples of platy-ridged lava seen in Iceland.

4. Some Other Examples of Platy-Ridged Lava in Iceland

[52] While the 1783–1784 Laki Flow Field is unique in having detailed eyewitness accounts of its emplacement, there are a number of additional examples of other platy-ridged lava flows in Iceland. Two we examined briefly are the Búrfells Lava near Lake Myvatn and a flow extending south from the Krafla Caldera. These reveal additional aspects of the formation of platy-ridged lava surfaces.

4.1. General Description of Búrfells Lava Flow Field

[53] The Búrfells Lava Flow Field is located in north-central Iceland, due east of Lake Myvatn and due south of Krafla Volcano (Figure 14). It is ~3000 years old and covers approximately 100 km². The lava appears to have been erupted from fissures on the east side of the flow field and have mostly flowed to the west. However, some lava flowed north and east from the now largely buried fissures [*Haack et al.*, 2002, 2004, manuscript in preparation, 2004].

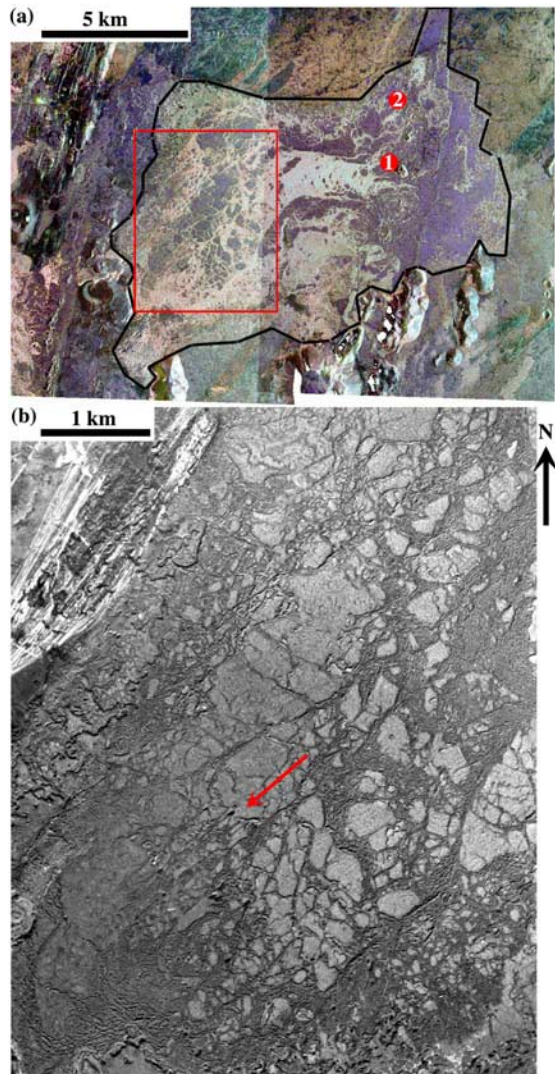[54] Both aerial and radar images of the area show plates, ridges, and grooves like those seen on Mars

Figure 15. Aerial images of the Búrfells lava. (a) Radar image of Búrfells lava and surroundings [*Haack et al.*, 2002, 2004]. Bright areas are rough and dark areas are smooth at the radar wavelengths (cm-dm). Red box shows location of air photo, and numbers in red refer to localities investigated in some detail in the field. The pattern of plates and ridges supports the suggestion that the vent for the Búrfells lava was a fissure on the east side of the flow field. (b) Air photo of the western side of the flow. The exteriormost ~500 m of the flow shows classic inflated lava textures (inflation plateaus and pits). The red arrow shows the location of a series of wakes in the lava and the indicated flow direction. While the wakes are ~1 km long, there is little shear that can be seen between the plates. This suggests that at least a 3 km wide extent of the flow top was moving in concert.

(Figure 15) [*Haack et al.*, 2004]. The plates have relatively smooth surfaces and range in size from ~100 m to ~2 km and are mostly bounded by topographically high ridges. The center of the flow field consists of a 1.5 km wide, 3.5 km long zone composed almost exclusively of ridges. From the orientation of the ridges and the surrounding plates, it appears that this is a zone of concentrated westward flow [*Haack et al.*, 2004, manuscript in preparation, 2004]. While this zone must mark the primary lava transport within the flow field, the term "channel" may not be appropriate to describe a feature with this aspect ratio. We prefer the term "sheet flow," but this should not be confused with pahoehoe sheet flows, which have stationary upper crusts. We will use the phrase "sheet flow with a mobile upper crust" when we need to avoid this confusion.

[55] As in the case of the Laki Flow Field, the margins of the Búrfells Lava Flow Field generally consist of inflated pahoehoe, as evidenced by tumuli, inflation pits, and inflation plateaus. This pahoehoe margin is typically ~100 m wide. Where examined in the field, the flow margin had inflation features tens of meters in lateral extent and 2–5 m in height. Grooves similar to those seen at Laki are prominent in the Búrfells lava, but they are shorter (500 m long at Búrfells compared to 1.5 km at Laki). In this paper, we describe two near-vent localities. Further field descriptions and interpretation of remote sensing data are given by H. Haack et al. (manuscript in preparation, 2004).

4.2. Detailed Morphology of Platy-Ridged Facies of the Búrfells Lava Flow Field

[56] The first field locality (labeled 1 in Figure 15) is in the immediate vicinity of one of the larger spatter mounds that built along the eruptive fissure. From this vantage point, it is possible to see one of the major differences between the platy-ridged lava at Búrfells and Laki: some of the prominent smooth lava surfaces are highstanding at Búrfells (Figures 16a and 16b). Both smooth plates and ridges composed of large slabs of lava are found at a lower topographic level. The remote sensing and field observations show that that the main Búrfells lava has surfaces at two distinct topographic levels.

[57] The lavas surrounding the spatter mound also have smooth plateaus at a higher topographic level than the platy-ridged lavas (Figures 16c and 16d). The sides of the plateaus reveal that they are composed of stacks of "shelly" pahoehoe (defined by a thin solid upper shell on a hollow lobe). Shelly
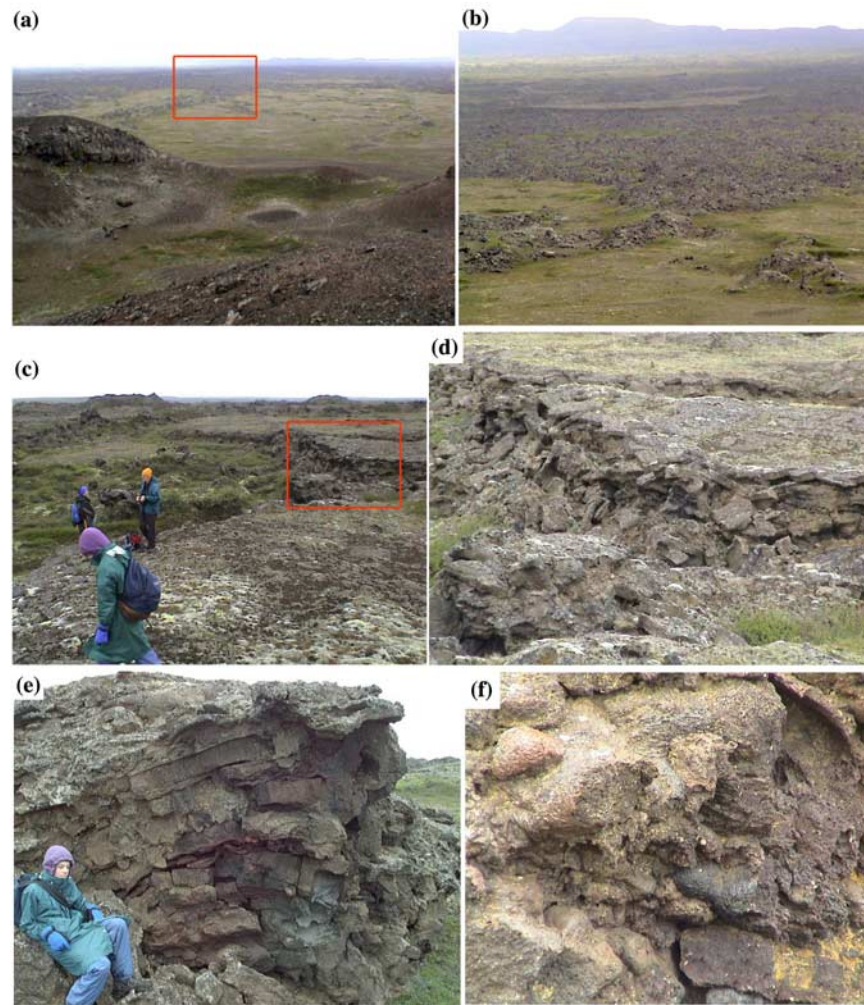
Figure 16. Photos of the near-vent region of the Búrfells lava. (a) View looking west from location 1 in Figure 14. Flat plates and ridges of breccia can be seen extending toward the horizon. (b) Close-up (red box in Figure 16a) of plates and ridges. Note that some plates are highstanding and others are lower than the ridges. (c) The margin of a highstanding plate. The surface of the plate is a smooth sheet of pahoehoe. (d) Close-up of red box in Figure 16c showing that the plate is composed of stacks of thin shelly pahoehoe flows. In Hawaii, stacks of shelly lavas are a common near-vent feature where a lava pond repeatedly overflows in thin, fluid sheets of liquid lava. (e) Another cliff of stacked shelly lava flows. Red zones with baking suggest a hiatus in the building of this stack. (f) Close-up of another lava scarp, this time consisting of pahoehoe lobes and thin slabs. This suggests smaller, less continuous flows building the stack of lavas. In all of these cases, it appears that the vertical scarp was created when liquid lava drained away, collapsing the surface of a lava lake.

pahoehoe is characteristic of near-vent lavas and often (but not always) form when the hot, fluid, interior of the lobe is able to drain out from under the solidified crust [*Swanson*, 1973]. The high vesicularity of these lavas also indicates that they froze while still near the vent. The lobes have 30–70 vol.%, 0.1–3 mm diameter vesicles at a density of 8–15 vesicles per cm^2. This is very similar to the vesicularity of the spatter in this area (70 vol.%, 0.1–2 mm diameter vesicles with a density of ~100 vesicles/cm^2). The shelly pahoehoe lobes that make up the plateaus are generally 50–

100 cm thick, 1–3 m wide, and have a ~20 cm thick upper crust. They often have ropey surfaces and red (oxidized) contacts (Figures 16e and 16f).

[58] This kind of stacking of near-vent lavas is a common feature of perched lava ponds [*Swanson*, 1973; *Carr and Greeley*, 1980]. Small pulses in effusion rate lead to small overflows from the growing lava pond, gradually building a levee around the pond. If the levee fails at some point, the lava drains away, exposing the stacks of small pahoehoe lobes of the remaining levee. These new

Figure 17. Ridges on the Búrfells and Krafla lavas. (a) Pressure ridges near location 2 in Figure 14. Note car in the background for scale. Many of the blocks in the pressure ridges here are fragments of slabs that were originally 50–80 cm thick. The plates between the pressure ridges have the same undulations seen in the Laki lava. (b) Close-up of slabs in the pressure ridge that form angular cavities that can efficiently reflect radar energy. Note pocketknife for scale. (c) Contact between brecciated and smooth surface within a lava flow on the southern side of Krafla. Note that the smooth lava has shallow drained tumuli and a classic pahoehoe surface. (d) Close-up of the margin of the breccia. The transition to the brecciated surface is not a change in lava flows. The breccia consists of slabs of exactly the same lava as the smooth surface in front of it. Slab thicknesses vary from 10 to 50 cm. Some slabs exhibit scrape marks, indicating that the brecciation took place while some of the lava was hot and plastic. Notebook for scale.

field observations support the conclusions from earlier studies that suggest that much of the Búrfells Lava Flow Field was a perched lava pond [*Haack et al.*, 2002, 2004].

[59] The second field locality (labeled 2 in Figure 15) is a few hundred meters from the fissure vent and the margin of the Búrfells Lava Flow Field. Figures 17a and 17b show typical ridge materials from the topographically lower, platy-ridged surface. The ridges here (and at locality 1) are almost exclusively composed of pahoehoe slabs. Most of the ridges contain slabs 50–80 cm thick, but some of the tallest ridges are composed of pieces of pahoehoe up to 2 m thick. In one case, an entire 1.5 m thick inflated pahoehoe sheet lobe was found within a tilted slab. There is no evidence of draining or plastic deformation of the lobe, indicating that it must have been completely solidified before being tilted. Other thick slabs have surfaces composed of slab pahoehoe, indicating at least 2 widely spaced episodes of disruption. The "smooth" plates between the ridges are also often com-

posed of slab pahoehoe. The slabs on the plates and thick slabs are only 10–20 cm thick. The plates also have upwarped regions bounded by polygonal fractures. As at Laki, these polygons are generally 3–5 m wide and are 10–15 cm higher in the center than at the margins.

[60] We interpret these observations as indicative of a complex mix of classic pahoehoe and slab pahoehoe lobes of different ages before the formation of the large ridges. For the 1.5 m pahoehoe lobe to have solidified, the *Hon et al.* [1994] model requires at least a week. The 50–80 cm thick slabs are indicative of 2–4 days of cooling. The formation of the ridges clearly involved compression, probably related to the catastrophic draining of the lava pond suggested by the remote sensing observations and features at locality 1.

4.3. Brief Description of Krafla Platy-Ridged Lava

[61] We briefly examined a well-exposed platy-ridged lava at the southern entry to Krafla Caldera.

This flow showed a sharp transition from a smooth, pahoehoe surface to a brecciated ridged surface (Figure 17c). The pahoehoe surface is more distal and shows a classic pahoehoe texture with stretched vesicles and ropes. The area shown in Figure 17c is the surface of a large inflation plateau with 5–10 m diameter inflation pits. A slightly drained tumulus provides a cross-sectional view into the upper crust which shows the typical vertical vesicle distribution seen in inflated pahoehoe flows, changing from ∼60 vol.% vesicles at the surface to ∼30 vol.% at a depth of 33 cm. The vesicles also become fewer and larger with depth, with vesicle shapes transitioning from stretched at the surface to round in the upper 10 cm to irregular at greater depth as the vesicles coalesce.

[62] The ridge material is dominated by slabs of pahoehoe crust. The larger slabs have ropes and even small pahoehoe lobes on one of their surfaces and frozen drips on the opposite side. The vertical vesicle distribution within these slabs is identical (in terms of volume fraction, number density, and vesicle shape) to that seen in the pahoehoe surface. In some cases, the lower sides of the slabs have parallel grooves imprinted into them. These are interpreted to be scrape marks made into the still hot and plastic lava as it moved past more rigid protrusions. The slabs are most often 1–2 m across, but one slab is 3 × 4 m across. The most common thickness is ∼50 cm, but some 10–15 cm thick slabs are also present. There are also rare fragments of 20–30 cm scale pahoehoe lobes.

[63] We interpret these observations to again show evidence for the break-up of a pre-existing pahoehoe surface by compressional forces. In this case, there seems to be only one episode of brecciation, but the original surface was composed of materials ranging in age from a few hours to nearly 2 days. There is no evidence for intrusion of any significant amount of fluid lava into this breccia. In this case, we cannot positively determine if lava flow inflation took place before or after the brecciation event (or both). However, the lack of inflation pits in the "ridge" material suggests that the inflation was primarily before the disruption of the crust.

5. Comparison of the Icelandic Platy-Ridged Lava Flows

[64] Having examined 3 different "platy-ridged" lava flows in Iceland, we attempt to draw some initial generalizations. However, the variety of lava features in the plates and ridges on the lava flows we described indicates that a variety of different processes are involved. By identifying the features that are consistent between the different examples, we start the process of creating a general conceptual model for how platy-ridged lavas are formed. However, we are very aware of the fact that we have not examined enough of these types of lava flows to reach definitive conclusions.

5.1. Similarities

[65] Perhaps the most striking similarity of these flows is that all the examples we have examined involve the disruption of an initial pahoehoe surface. The clasts in the breccias are in all cases dominated by either slabs of pahoehoe crust or disrupted pieces of pahoehoe lobes. Furthermore, all the margins of these flows are composed primarily of inflated pahoehoe.

[66] At this point, it is not clear if an aa flow can form a platy-ridged surface. Ridges of breccia oriented perpendicular to flow are indeed a common feature in aa flows. Furthermore, given that an aa surface is already brecciated, it may be difficult to recognize the presence of "plates" in such a flow. Further fieldwork is needed to empirically determine if the processes that form platy-ridged lavas are exclusively tied to the pahoehoe emplacement process.

[67] Another common feature of all the platy-ridged flows examined in Iceland is that the ridges were formed by compression of the lava flow top. This requires the shortening of the existing upper lava surface and the generation of new flow top material. It is usually not clear where and how this new crust is formed. Only at locality 1 in the Laki Flow Field do we have clear evidence for the formation of new crust. In that case, we see that fluid lava welled up into the gap left in the upper crust, both in the grooves and in space between plates that separated. In the other localities, we suspect that the new crust was forming upflow of the ridges at a rate faster than the flow front was advancing. This would provide ridges with the necessary extra material and leave few preserved features. The question of how new crust forms on platy-ridged flows clearly requires further study.

[68] A smaller feature that is found on both the Laki and Búrfells Flow Fields are the upwarped mounds with polygonal margins on the smooth lavas. Such features are also common on Hawaiian lava lakes. The polygonal fractures are probably caused by cooling and the sagging along the

fractures could be a result of gas escape. Bubbles would be trapped at the center of each of the polygons, but some gas could escape along the fractures. The result would be a slight decrease in the volume of the lava adjacent to the fractures, causing the polygon to warp. We feel that the presence of these features suggests that these lava flows may have spent a significant period of time acting like quiescent lava ponds.

5.2. Differences

[69] To date, we have found two fundamental differences in the examples of platy-ridged lava in Iceland. The first is in the detailed nature of the materials in the flow top breccias. The second is related to the mechanisms that produced the compression that created the ridges. A less important difference is the presence or absence of inflation after flow top brecciation. This shows that these lava flows can return to behaving like pahoehoe sheet flows after the brecciation event(s), rather than elucidating the processes that form the platy-ridged flow morphology.

[70] The difference in the materials making up the flow top breccia at localities 1, 2, and 3 of the Laki Flow Field and the other three areas we described is striking. In the main part of the Laki Flow Field, the breccia is composed primarily of broken and/or contorted pahoehoe lobes. Slabs of pahoehoe and coherent blocks of breccia also exist, but are not the dominant material. In the other areas, the breccia is dominated by slabs of relatively flat pahoehoe surfaces. It is not possible to attribute these differences to just the fact that vertical cuts into the breccia were available only in the main part of the Laki Flow Field. The difference in the clasts in the breccias is evident at the surface. Other differences are that the flow top breccia seems to be thicker at localities 1, 2, and 3 from Laki than in the other areas (4–5 m thick vs. 0.5–2 m), and the presence of intrusions of the underlying liquid lava into the breccia only in the main part of the Laki Flow Field.

[71] After reviewing all the field evidence, we propose that this difference is primarily a result of the brecciation event being more extended in time in the case of the main Laki Flow Field. There is compelling evidence that the breccia at Laki must have formed over a significant period of time. There are plastically deformed clasts that have had other clasts wrap around them after the initial clast had hardened. If exposed at the surface, these 10-cm scale clasts could harden in about an hour.

However, these clasts are found deep in the breccia, where cooling should have been significantly slower. This suggests that the 4–5 m thick flow top breccia at Laki took at least hours to form. However, the eyewitness accounts of the Laki eruption preclude having the breccia form over many days.

[72] We furthermore propose that the formation of a breccia composed predominantly of slabs is the first stage of a continuum of processes that produce platy-ridged lava flows. These slab-dominated breccias seem to have formed in a single short-lived event. Continued brecciation breaks the slabs into more equant pieces and causes mixing with the fluid interior. This process would also thicken the flow top breccia. Thus, we suggest that if the brecciation had continued for longer, the surfaces at locality 4 on the Laki Flow Field, the Búrfells Lava Flow Field, and the Krafla example we discussed would all have become like the main part of the Laki Flow Field.

[73] The fundamental difference in emplacement style of the Búrfells and Laki Flow Fields probably explains why brecciation was sustained for such different time spans. At Laki, the lava sheet was fed by a long-lived eruption with surges that were sustained for days to weeks. At Búrfells, it seems that a very large perched lava pond was suddenly drained near the end of the eruption. At locality 4 on the Laki Flow Field and in the Krafla locality, we appear to be dealing with a relatively small and short-lived lobe. Thus, we suspect that the detailed nature of the flow top breccia can provide important insight into the nature of the eruption that produced that particular platy-ridged lava flow.

6. Discussion

6.1. Revising the Conceptual Model for the Formation of Platy-Ridged Lavas

[74] These new field observations allow us to refine our initial conceptual model for the formation of platy-ridged lava flows presented by *Keszthelyi et al.* [2000]. The evidence supports our initial hypothesis that these flows are generated when the originally coherent upper surface of the lava flow is disrupted by a large flux of lava within the flow. However, the new field observations do show that the brecciation process is more complex than we had initially envisioned.

[75] Figure 18 provides a simplified cartoon of this process, as we currently understand it. We see three
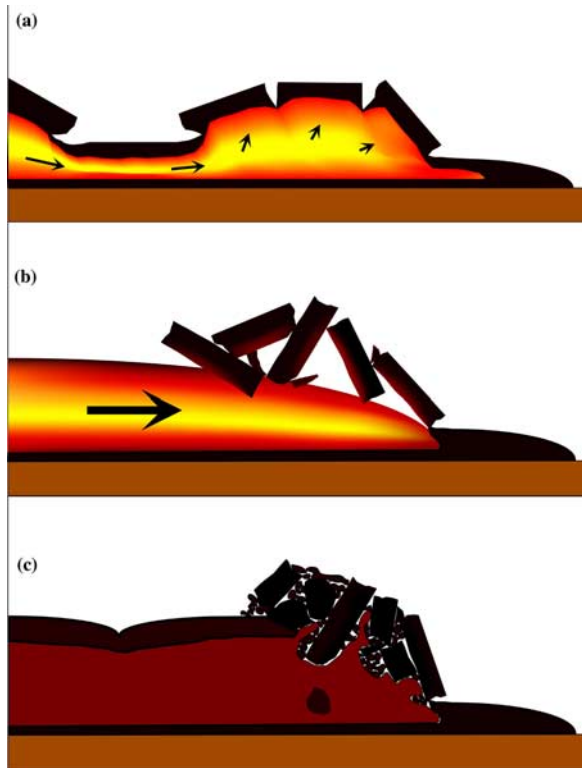
Figure 18. Schematic diagram of the formation of platy-ridged (rubbly pahoehoe) lava flows. (a) It appears that the flow is initially emplaced as an inflating pahoehoe sheet flow. Tumuli and other classic inflation features form in the manner described by *Hon et al.* [1994]. (b) At some point the flux of lava overpowers the strength of the upper crust and begins to carry the surface on top of the moving lava. Locally, the crust breaks and compresses into pressure ridges. These initial pressure ridges are composed of slabs of pahoehoe that are typically many tens of centimeters thick and have large void spaces within them. (c) Continued flux of lava can continue to transport the flow top, increasing the brecciation of the initial pahoehoe slabs, building the large breccia ridges. Liquid lava intrudes the breccia from below in the form of meter-scale pahoehoe lobes. These intruding lobes can also be disrupted (while solid, plastic, or liquid) by the motion within the breccia, producing a new generation of breccia clasts. These secondary clasts are commonly a few tens of centimeters in scale and characterized by contorted shapes. Also, in between the ridges of breccia, new smooth pahoehoe surfaces can form. These new smooth surfaces behave like the surfaces of lava lakes, forming polygonal fractures on a 10-m scale. Martian flood lavas can be seen frozen with morphology corresponding to each of these stages in the development of platy-ridged lava. In fact, some flows show evidence for yet another stage of brecciation, where plates of ridged material are mobilized by lava flowing beneath the flow top.

main phases in the formation of platy-ridged lava. First, a pahoehoe flow is emplaced. This pahoehoe flow forms a coherent, insulating crust that is only broken by cooling fractures and differential inflation. While the crust may locally be lifted or tilted, it is not translated for any significant distance. In the second stage, the crust is disrupted and carried away by a large influx of liquid lava into the interior of the lava flow. This high flux can be supplied by a surge in the effusion of lava at the vent or by processes internal to the lava flow (for example, the failure of the margins of a ponded lava flow). The product of this disruption is a flow top with ridges composed of buckled slabs of pahoehoe crust and smooth pahoehoe surfaces that have been translated laterally as coherent plates. By the end of this second stage, a platy-ridged lava morphology has been formed. However, in some cases, the flow continues into a third phase. This phase involves a sustained disruption of the flow top, breaking the pahoehoe slabs into more equant pieces and injecting new lava into the flow top breccia. If this process is sustained for long enough (or repeated often enough), the breccia becomes dominated by contorted pieces of broken pahoehoe. Ridges continue to form in the breccia where there is net shortening of the flow top and new smooth pahoehoe surfaces form where the interior of the flow is exposed. In some cases, the flow may enter a phase of inflation before final solidification.

6.2. Are "Platy-Ridged Lava" and "Rubbly Pahoehoe" the Same?

[76] It would be strange if these platy-ridged lavas were confined, on Earth, to only Iceland. In fact, the descriptions of the breccia from the main part of the Laki Flow Field are identical to that of breccias we have seen in continental flood basalt provinces. While not the dominant type of flow surface, brecciated flows are not uncommon in the Columbia River Basalts [*Self et al.*, 1998]. These breccias do not contain classic aa clasts. Instead, they are composed of contorted and broken pieces of pahoehoe [*Keszthelyi*, 2000; *Keszthelyi et al.*, 2001]. We have informally called these flows "rubbly pahoehoe" because their surfaces are composed of pahoehoe "rubble." The examples in the Columbia River Basalts are mostly lava flows ∼40 m thick with 4−5 m thick flow top breccias. Smaller examples were found to be common in drill core from the subaerial lavas of the Kerguelen Plateau [*Coffin et al.*, 2000; *Keszthelyi*, 2002].

Table 4. Terms Used in Thermal Model for Martian Platy-Ridged Lava Flows

Symbol	Explanation	Value Used
$\partial T/\partial x$	cooling per distance traveled	see Table 5
Q_{visc}	heat added to the core of the flow by viscous dissipation	
Q_{rad}	heat loss from the core of the flow by thermal radiation	
Q_{atm}	heat loss from the core of the flow by atmospheric convection	
Q_{entr}	heat loss from the core of the flow by entrainment of crust	
$\langle \mathbf{v} \rangle$	mean flow velocity of the core of the lava flow	
ρ	density of the lava (corrected for vesicles)	2080 kg/m^3
C_p^*	heat capacity of the lava (corrected for crystallization)	2775 J/kg °C
H	thickness of lava flow core	20 m
g	gravitational acceleration	3.7 m/s^2
θ	slope	0.03%
ε	emissivity	0.95
σ	Stephan-Boltzmann constant	5.67×10^{-8}
f	fraction of lava core exposed (not covered by crust)	see Table 5
T	lava temperature	1100 °C
T_a	ambient temperature	−70 °C
$\mathbf{h}$	atmospheric heat transfer coefficient	2 W/m^2 °C
H_{c}	thickness of upper crust	see Table 5
T_c	average temperature of crust	see Table 5
τ	time a piece of crust avoids entrainment	see Table 5
η	viscosity	1000 Pa s

[77] While the breccias in rubbly pahoehoe and some platy-ridged lava flows appear indistinguishable, it is not yet proven that the two are identical. In particular, the rubbly pahoehoe seen in the flood basalts have all come from outcrops of relatively limited lateral extent. As such, we have not yet found convincing evidence that rubbly pahoehoe flow surfaces have a combination of smooth plates and ridges. However, if the connection between rubbly pahoehoe and platy-ridged lava can be made, then we can apply the conceptual model derived from Iceland to these continental flood basalt lava flows. Preliminary studies suggest that these flows may have been emplaced in a very rapid, but laminar flow regime [*Keszthelyi et al.*, 2003]. If correct, this work suggests that these particular flows may have involved eruption rates large enough to inject volcanic gases directly into the stratosphere and potentially have an impact on global climate [*Keszthelyi et al.*, 2001].

6.3. Improved Emplacement Model for Martian Flood Lavas

[78] We can use the new field observations to improve the calculations presented in *Keszthelyi et al.* [2000] on the thermal efficiency of platy-ridged lava flows on Mars. The *Keszthelyi et al.* [2000] model used a modification of the *Crisp and Baloga* [1994] thermal model for large aa flows that was described in detail by *Keszthelyi and Self*

[1998]. This model estimates cooling along the length of a flow by summing the terms in the thermal budget. The model can be summarized with the following equations:

$$\partial T/\partial x = (Q_{\text{visc}} - Q_{\text{rad}} - Q_{\text{atm}} - Q_{\text{entr}})/\left(\langle \mathbf{v} \rangle \rho \, C_p^* H\right),$$

$$Q_{\text{visc}} = \rho \, g \, H \langle \mathbf{v} \rangle \theta,$$

$$Q_{\text{rad}} = \varepsilon \sigma f \left(T^4 - T_a^4\right),$$

$$Q_{\text{atm}} = \mathbf{h} \, f (T - T_a),$$

$$Q_{\text{entr}} = \rho \, C_p^* H_{\text{c}} (T - T_c)/\tau,$$

$$\langle \mathbf{v} \rangle = \rho \, g \, \theta \, H^2/3 \, \eta,$$

where the terms are defined in Table 4. Key simplifying assumptions are that the flow is in thermal steady state and that the lava behaves as a Newtonian fluid flowing down an inclined plane. With these significant simplifications, only broad conclusions can be drawn about the lava as it moves from near the vent to near the flow front.

[79] The field observations from Iceland give us some more realistic values for the behavior of

Table 5. Results From Thermal Model Using Different Crust Properties[a]

Crust Type	f, %	H_c, m	T_c, °C	τ, s	$\partial T/\partial x$, °C/km	Length, km
Thick Laki	0.01	5	700	10^6	0.43	120
Búrfells	1	1	700	10^5	0.74	68
Early 1984	10	0.02	700	300	4.9	10
Late 1984	1	1	400	10^5	1.3	38
"Thin"	50	0.05	1000	10^2	11	4.5
"Medium"	10	1	600	10^3	86	0.58
"Thick"	1	10	400	10^5	23	2.2

[a] "Thin," "medium," and "thick" crust types refer to cases from *Keszthelyi et al.* [2000].

disrupted crust than what was available previously. Table 5 lists the range of input parameters we have examined here. We examine the thermal efficiency of the thick breccias seen on the main part of the Laki Flow Field and the thinner breccias on the Búrfells Lava. For comparison, we also show results for the 1984 Mauna Loa aa flow and the model runs examined by *Keszthelyi et al.* [2000]. We assume that the lava flow will stop after the core cools approximately 50°C [*Keszthelyi and Self*, 1998].

[80] These results show that platy-ridged lava flows are about 2 orders of magnitude more thermally efficient than we had estimated by *Keszthelyi et al.* [2000]. The modeling of *Keszthelyi et al.* [2000] suggested that platy-ridged lavas could have advanced only a short distance (a few tens of kilometers) under the most favorable circumstances. The new data from Laki indicates that this type of lava flow is actually capable of advancing >100 km while producing the platy-ridged morphology. This indicates that the length of the Laki Flow Field was limited by flow volume, not cooling. This modeling supports the contention that the Laki eruption had the potential to be as large as continental flood basalt flows, if initial eruption rates were sustained [e.g., *Self et al.*, 1997; *Thordarson and Self*, 1998]. The flow velocities on Mars predicted by this model are of order 0.3 m/s for a 20 m thick flow. For the ~50 km wide Martian flood lava flows, it implies an effusion rate of ~3 × 10^5 m³/s.

[81] These intriguing results, from a very simplistic thermal model, invite more thorough modeling efforts. In particular, the assumption that the flow will behave as a Newtonian fluid is in need of improvement. Our analysis of the rheology of the Laki lavas suggests that the strain rate dependence of the effective viscosity of lava cannot be ignored. The constant value of 1000 Pa s that we used here is probably a good

approximation of the average value for the entire flow. However, depending on how the shear is distributed within the flow, the actual flow velocities could be as much as an order of magnitude higher or lower than we calculated here. The assumption of steady state is also in need of re-evaluation, especially in the case that the platy-ridged morphology may have formed in a short-lived event.

6.4. Implication for Future Mars Missions

[82] The Cerberus plains were seriously considered as a landing site for the Mars Exploration Rovers, but the site was rejected because of fears that the surface was too rough for safe landing or driving. Our field observations confirm that there is reason for grave concern for any future mission that might land on pristine platy-ridged lava flows. Plates are probably some of the smoothest surfaces we can find, ridges some of the roughest. A precision landing capability to avoid the ridges is required to land within this type of surface. Landing at the margin of this type of flow and climbing onto it is also a difficult proposition. Therefore the study of pristine examples of platy-ridged lava flows on Mars will probably have to continue to be primarily based on remote sensing observations from orbit.

7. Conclusions

[83] We have conducted detailed field investigations of Icelandic lava flows that show the same surface morphology as Martian platy-ridged flood lavas. These flows have flow top breccias composed of disrupted pahoehoe lava. In some cases, the disruption is quite limited and the breccia consists of simple slabs of pahoehoe. In other cases, the disruption appears to have been sustained over a longer period of time. In these locations, the breccia is dominated by contorted

pieces of broken pahoehoe lobes. Intact pahoehoe lobes, slabs of pahoehoe crust, and intrusions of fluid lava from below can also be found in these breccias. Spinose aa clasts are extremely rare. The margins of the flows were almost exclusively inflated pahoehoe.

[84] From these observations, we conclude that the platy-ridged lava morphology is formed in a multistage process. First, a pahoehoe sheet flow is emplaced. Hours to days after emplacement of the sheet flow, a large flow of liquid lava within the sheet disrupts and carries away the solidified crust. Ridges of pahoehoe slabs form as pressure ridges where the crust undergoes local shortening. This flow of liquid lava can be caused either by surges in effusion rate at the vent, or by large breakouts from the sheet flow (i.e., the catastrophic failure of the margins of a ponded flow). If the flux of lava is sustained, then the brecciation process can continue for an extended period of time. In this case, the breccia can evolve from simple slabs to a mix of broken and contorted pahoehoe lobe fragments that have been cooling for different periods of time.

[85] A simple thermal model utilizing the field observations from Iceland shows that these platy-ridged lava flows may be far more thermally efficient than had been inferred from the earlier *Keszthelyi et al.* [2000] work. This allows the Martian flood lavas to have been emplaced largely in a mode where the upper crust was being continually disrupted as it was carried on top of the sheet of liquid lava. A similar process may have been involved in the emplacement of some continental flood basalt lava flows on Earth that exhibit a ''rubbly pahoehoe'' flow top breccia. The modeling also suggests that these flows may have been fed by very high effusion rate eruptions ($\sim 10^5$ m^3/s) but the flow would have still moved in the laminar regime.

[86] While we have succeeded in shedding some new light on how many Martian flood lavas were emplaced, this work also highlights the need for several future studies. The simple thermal model needs to be improved, especially in regard to using more realistic lava rheologies. The possible link between the rubbly pahoehoe flows seen in terrestrial flood basalt provinces and the platy-ridged mode of lava emplacement also needs to be pursued with more field studies. It is likely that examining terrestrial lava flows that are more similar in scale to the Martian flood lavas will lead to new insights. Finally, one avenue of future study,

the driving of rovers on pristine Martian platy-ridged lava flows, seems essentially impossible.

References

Arkani-Hamed, J., and L. Riendler (2002), Stress differences in the Martian lithosphere: Constraints on the thermal state of Mars, *J. Geophys. Res.*, *107*(E12), 5119, doi:10.1029/2002JE001851.

Asimow, P. D., and M. S. Ghiorso (1998), Algorithmic modifications extending MELTS to calculate subsolidus phase relations, *Am. Mineral.*, *83*, 1127–1131.

Berman, D. C., and W. K. Hartmann (2002), Recent fluvial, volcanic, and tectonic activity on the Cerberus plains of Mars, *Icarus*, *159*, 1–17.

Beyer, R. A. (2004), Martian surface roughness and stratigraphy, Ph.D. thesis, Univ. of Ariz., Tucson.

Bottinga, Y., and D. F. Weill (1972), The viscosity of magmatic silicate liquids: A model for calculation, *Am. J. Sci.*, *272*, 438–475.

Burr, D. M., J. A. Grier, A. S. McEwen, and L. P. Keszthelyi (2002), Repeated aqueous flooding from the Cerberus Fossae: Evidence for very recently extant, deep groundwater on Mars, *Icarus*, *159*, 53–73.

Carr, M. H., and R. Greeley (1980), *Volcanic Features of Hawaii: A Basis for Comparison With Mars*, 211 pp., NASA, Washington, D. C.

Cashman, K. V., and J. P. Kauahikaua (1997), Re-evaluation of vesicle distributions in basaltic lava flows, *Geology*, *25*, 419–422.

Chapman, M. G. (1999), Elysium Basin lava flows: New interpretations based on MOC data (abstract), *Proc. Lunar Planet. Sci. Conf. 30th*, abstract 1279.

Christensen, P. R., J. L. Bandfield, M. D. Smith, V. E. Hamilton, and R. N. Clark (2000), Identification of a basaltic component on the Martian surface from Thermal Emission Spectrometer data, *J. Geophys. Res.*, *105*, 9609–9622.

Christensen, P. R., et al. (2003), Morphology and composition of the surface of Mars: Mars Odyssey THEMIS results, *Science*, *300*, 2056–2061.

Coffin, M. F., et al. (2000), *Proceedings of the Ocean Drilling Program, Initial Reports*, vol. 183, *Kerguelen Plateau-Broken Ridge, Sites 1135–1142, 7 December 1998–11 February 1999*, 101 pp. + CD-ROM, Ocean Drill. Program, College Station, Tex.

Crisp, J., and S. M. Baloga (1994), Influence of crystallization and entrainment of cooler material on the emplacement of basaltic aa flows, *J. Geophys. Res.*, *99*, 1819–1831.

Frey, H., and R. A. Schultz (1988), Large impact basins and the mega-impact origin for the crustal dichotomy on Mars, *Geophys. Res. Lett.*, *15*, 229–232.

Frey, H. V., J. H. Roark, K. M. Shockey, E. L. Frey, and S. E. H. Sakimoto (2002), Ancient lowlands on Mars, *Geophys. Res. Lett.*, *29*(10), 1384, doi:10.1029/2001GL013832.

Fuller, E. R., and J. W. Head III (2002), Amazonis Planitia: The role of geologically recent volcanism and sedimentation in the formation of the smoothest plains on Mars, *J. Geophys. Res.*, *107*(E10), 5081, doi:10.1029/2002JE001842.

Ghiorso, M. S., and R. O. Sack (1995), Chemical mass transfer in magmatic processes. IV. A revised and internally consistent thermodynamic model for the interpolation and extrapolation of liquid-solid equilibria in magmatic systems at elevated temperatures and pressures, *Contrib. Mineral. Petrol.*, *119*, 197–212.

Ghiorso, M. S., M. M. Hirschmann, P. W. Reiners, and V. C. Kress III (2002), The pMELTS: A revision of MELTS for improved calculation of phase relations and major element partitioning related to partial melting of the mantle to 3 GPa, *Geochem. Geophys. Geosyst.*, *3*, 1030, doi:10.1029/2001GC000217.

Greeley, R., and J. E. Guest (1987), Geologic map of the eastern equatorial region of Mars, *U. S. Geol. Surv. Misc. Invest. Ser.*, Map I-1802-B.

Greeley, R., and J. S. King (1977), *Volcanism of the Eastern Snake River Plain, Idaho: A Comparative Planetary Geology Guidebook*, 308 pp., NASA, Washington, D. C.

Haack, H., M. Rossi, and A. Höskuldsson (2002), Búrfellshraun: A SAR study of a unique volcanic eruption (abstract), paper presented at 25th Nordic Geologic Winter Meeting, Reykjavik, 6–9 Jan.

Haack, H., J. Dall, and M. Rossi (2004), Búrfellshraun: A terrestrial analog to recent volcanism on Mars (abstract), *Proc. Lunar Planet. Sci. Conf. 35th*, abstract 1468.

Hartmann, W. K., and D. C. Berman (2000), Elysium Planitia lava flows: Crater count chronology and geological implications, *J. Geophys. Res.*, *105*, 15,011–15,026.

Hartmann, W. K., and G. Neukum (2001), Cratering chronology and the evolution of Mars, *Space Sci. Rev.*, *96*, 165–194.

Head, J. W., III, M. A. Kreslavsky, and S. Pratt (2002), Northern lowlands of Mars: Evidence for widespread volcanic flooding and tectonic deformation in the Hesperian Period, *J. Geophys. Res.*, *107*(E1), 5003, doi:10.1029/2000JE001445.

Head, J. W., L. Wilson, and K. L. Mitchell (2003), Generation of recent massive water floods at Cerberus Fossae, Mars by dike emplacement, cryospheric cracking, and confined aquifer groundwater release, *Geophys. Res. Lett.*, *30*(11), 1577, doi:10.1029/2003GL017135.

Hon, K., J. Kauahikaua, R. Denlinger, and K. McKay (1994), Emplacement and inflation of pahoehoe sheet flows: Observations and measurements of active flows on Kilauea Volcano, Hawaii, *Geol. Soc. Am. Bull.*, *106*, 351–383.

Keszthelyi, L. (2000), The brecciated lava flows of the Kerguelen Plateau: What are they?, *Eos Trans. AGU*, *81*(19), Spring Meet. Suppl, Abstract V41A-09.

Keszthelyi, L. (2002), Classification of mafic lava flows from ODP Leg 183 [online], *Proc. Ocean Drill, Program Sci. Results*, *183*. (Available at http://www-odp.tamu.edu/publications/183_SR/012/012.htm)

Keszthelyi, L., and R. Denlinger (1996), The initial cooling of pahoehoe flow lobes, *Bull. Volcanol.*, *58*, 5–18.

Keszthelyi, L., and S. Self (1998), Some physical requirements for the emplacement of long basaltic lava flows, *J. Geophys. Res.*, *103*, 27,447–27,464.

Keszthelyi, L., A. S. McEwen, and T. Thordarson (2000), Terrestrial analogs and thermal models for Martian flood lavas, *J. Geophys. Res.*, *105*, 15,027–15,050.

Keszthelyi, L., T. Thordarson, and S. Self (2001), Rubbly pahoehoe: Implications for flood basalt eruptions and their atmospheric effects (abstract), *Eos Trans. AGU*, *84*(47), Fall Meet. Suppl. Abstract V52A-1050.

Keszthelyi, L., T. Thordarson, and S. Self (2003), Quantitative assessment of models for the emplacement of the Columbia River Basalt lava flows (abstract), *Geol. Soc. Am. Abstr. Programs*, *35*, 136.

Kreslavsky, M. A., and J. W. Head (2000), Kilometer-scale roughness of Mars: Results from MOLA data analysis, *J. Geophys. Res.*, *105*, 26,695–26,711.

Lanagan, P., and A. S. McEwen (2004), Geomorphic analysis of the Cerberus plains: Constraints on the emplacement of the youngest lava flows on Mars, *Icarus*, in press.

Lenardic, A., F. Nimmo, and L. Moresi (2004), Growth of the hemispheric dichotomy and the cessation of plate tectonics on Mars, *J. Geophys. Res.*, *109*, E02003, doi:10.1029/2003JE002172.

Lodders, K. (1998), A survey of shergottite, nakhlite and chassigny meteorites whole-rock compositions, *Meteorit. Planet. Sci.*, *33*, A183–A190.

McEwen, A. S., M. C. Malin, M. H. Carr, and W. K. Hartmann (1999), Voluminous volcanism on early Mars revealed in Valles Marineris, *Nature*, *397*, 584–586.

McGill, G. E., and A. M. Dimitriou (1990), Origin of the Martian global dichotomy by crustal thinning in the late Noachian or early Hesperian, *J. Geophys. Res.*, *95*, 12,595–12,605.

Nyquist, L. E., D. D. Bogard, C.-Y. Shih, A. Greshake, D. Stöffler, and O. Eugster (2001), Ages and geologic histories of Martian meteorites, *Space Sci. Rev.*, *96*, 105–164.

Peterson, D. W., and R. I. Tilling (1980), Transition of basaltic lava from pahoehoe to aa, Kilauea Volcano, Hawaii: Field observations and key factors, *J. Volcanol. Geotherm. Res.*, *7*, 271–293.

Pinkerton, H., and R. Stevenson (1992), Methods for determining the rheological properties of lavas from their physicochemical properties, *J. Volcanol. Geotherm. Res.*, *53*, 47–66.

Plescia, J. B. (1990), Recent flood lavas in the Elysium region of Mars, *Icarus*, *88*, 465–490.

Plescia, J. B. (2003), Cerberus Fossae, Elysium, Mars: A source for lava and water, *Icarus*, *164*, 79–95.

Rice, J. W., T. J. Parker, A. J. Russell, and O. Knudsen (2002), Morphology of fresh outflow channel deposits on Mars, *Proc. Lunar Planet. Sci. Conf. 33rd*, abstract 2026.

Rice, J. W., P. R. Christensen, S. W. Ruff, and J. C. Harris (2003), Martian fluvial landforms: A THEMIS perspective after one year at Mars, *Proc. Lunar Planet. Sci. Conf. 34th*, abstract 2091.

Rossbacher, L. A., and S. Judson (1981), Ground ice on Mars: Inventory, distribution, and resulting landforms, *Icarus*, *45*, 39–59.

Scott, D. H., and K. L. Tanaka (1986), Geologic map of the western equatorial region of Mars, *U. S. Geol. Surv. Misc. Invest. Ser.*, Map I-1802-A.

Seibert, N. M., and J. S. Kargel (2001), Small-scale Martian polygonal terrain: Implications for liquid surface water, *Geophys. Res. Lett.*, *28*(5), 899–902.

Self, S., T. Thordarson, and L. Keszthelyi (1997), Emplacement of continental flood basalt lava flows, in *Large Igneous Provinces*, *Geophys. Monogr. Ser.*, vol. 100, edited by J. J. Mahoney and M. Coffin, pp. 381–410, AGU, Washington, D. C.

Self, S., L. Keszthelyi, and T. Thordarson (1998), The importance of pahoehoe, *Annu. Rev. Earth. Planet. Sci.*, *26*, 81–110.

Steingrímsson, J. (1998), *Fires of the Earth: The Laki Eruption 1783–1784*, translated by K. Kunz, pp. 1–95, Univ. of Iceland Press, Reykjavík.

Swanson, D. A. (1973), Pahoehoe flows from the 1969–1971 Mauna Ulu eruption, Kilauea Volcano, Hawaii, *Geol. Soc. Am. Bull.*, *84*, 615–626.

Takahashi, T. J., and J. D. Griggs (1987), Hawaiian volcanic features: A photoglossary, in *Volcanism in Hawaii*, edited by R. W. Decker, T. L. Wright, and P. H. Stauffer, *U.S. Geol. Surv. Prof. Pap.*, *1350*, 845–902.

Tanaka, K. L. (1986), The stratigraphy of Mars, *Proc. Lunar Planet. Sci. Conf. 17th*, Part 1, *J. Geophys. Res.*, *91*, suppl., E139–E158.

Tanaka, K. L., and D. H. Scott (1987), Geologic map of the polar regions of Mars, *U. S. Geol. Surv. Misc. Invest. Ser.*, *Map. I-1802-C*.

Tanaka, K. L., J. A. Skinner Jr., T. M. Hare, T. Joyal, and A. Wenker (2003), Resurfacing history of the northern plains of Mars based on geologic mapping of Mars Global Surveyor data, *J. Geophys. Res.*, *108*(E4), 8043, doi:10.1029/2002JE001908.

Thorarinsson, S. (1968), The Lakagigar eruption of 1783 and the Lakagigar crater row, *Natturufraedhingurinn*, *37*, 27–57.

Thordarson, T. (1995), Volatile release and atmospheric effects of basaltic fissure eruptions, Ph.D. thesis, 570 pp., Univ. of Hawaii Manoa, Honolulu.

Thordarson, T., and S. Self (1993), The Laki (Skaftár Fires) and Grímsvötn eruptions in 1783–1785, *Bull. Volcanol.*, *55*, 233–263.

Thordarson, T., and S. Self (1998), The Roza Member, Columbia River Basalt Group: A gigantic pahoehoe lava flow field formed by endogenous processes?, *J. Geophys. Res.*, *103*, 27,411–27,445.

Thordarson, T., S. Self, N. Óskarsson, and T. Hulsebosch (1996), Sulfur, chlorine, and fluorine degassing and atmospheric loading by the 1783–84 AD Laki (Skaftár Fires) eruption in Iceland, *Bull. Volcanol.*, *58*, 205–225.

Tolan, T. L., S. P. Reidel, M. H. Beeson, J. L. Anderson, K. R. Fecht, and D. A. Swanson (1989), Revisions to the estimates of the aerial extent and volume of the Columbia River Basalt Group, in *Volcanism and Tectonism in the Columbia River Flood Basalt Province*, edited by S. P. Reidel and P. R. Hooper, *Spec. Pap. Geol. Soc. Am.*, *239*, 1–20.

Williams, R. M. E., and M. C. Malin (2004), Evidence for late stage fluvial activity in Kasei Valles, Mars, *J. Geophys. Res.*, *109*, E06001, doi:10.1029/2003JE002178.

Woodworth-Lynas, C., and J. Y. Guigné (2003), Ice keel scour marks on Mars: Evidence for floating and grounding ice floes in Kasei Valles, *Oceanography*, *16*, 90–97.